

AD-A166 629

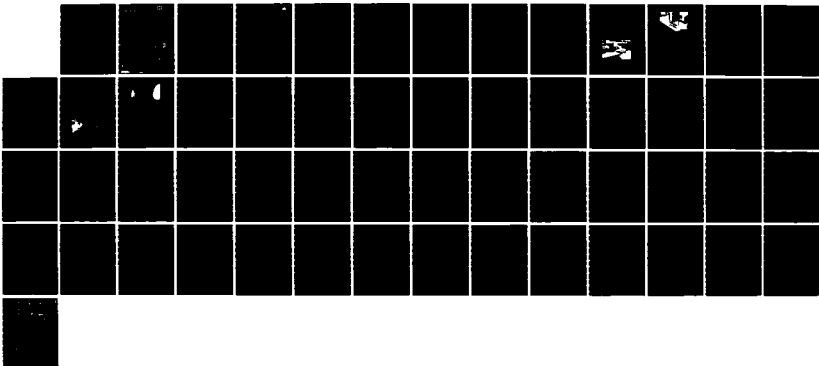
LEVEL ICE BREAKING BY A SIMPLE WEDGE(U) COLD REGIONS
RESEARCH AND ENGINEERING LAB HANOVER NH J TATINCLAUX
DEC 85 CRREL-85-22

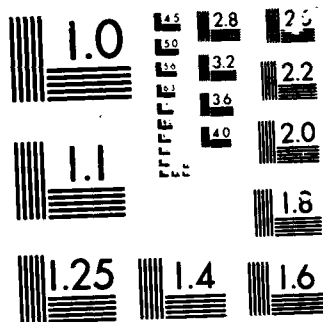
1/1

UNCLASSIFIED

F/G 8/12

NL





MICROCOPY

CHART

CRREL

REPORT 85-22



12

**US Army Corps
of Engineers**

Cold Regions Research &
Engineering Laboratory

Level ice breaking by a simple wedge

AD-A166 629

DTIC
ELECTE
APR 16 1986
S B D

DTIC FILE COPY

DISTRIBUTION STATEMENT A
Approved for public release
Distribution Unlimited

For conversion of SI metric units to U.S./British customary units of measurement consult ASTM Standard E380, Metric Practice Guide, published by the American Society for Testing and Materials, 1916 Race St., Philadelphia, Pa. 19103.

Cover: When the wedge is withdrawn, the breaking pattern in the ice is clearly seen.

CRREL Report 85-22

December 1985



Level ice breaking by a simple wedge

Jean-Claude Tatinclaux

Unclassified

SECURITY CLASSIFICATION OF THIS PAGE (When Data Entered)

REPORT DOCUMENTATION PAGE		READ INSTRUCTIONS BEFORE COMPLETING FORM								
1. REPORT NUMBER CRREL Report 85-22	2. GOVT ACCESSION NO. AD-A166 629	3. RECIPIENT'S CATALOG NUMBER								
4. TITLE (and Subtitle) LEVEL ICE BREAKING BY A SIMPLE WEDGE		5. TYPE OF REPORT & PERIOD COVERED								
		6. PERFORMING ORG. REPORT NUMBER								
7. AUTHOR(s) Jean-Claude Tatinclaux		8. CONTRACT OR GRANT NUMBER(s)								
9. PERFORMING ORGANIZATION NAME AND ADDRESS U.S. Army Cold Regions Research and Engineering Laboratory Hanover, New Hampshire 03755-1290		10. PROGRAM ELEMENT, PROJECT, TASK AREA & WORK UNIT NUMBERS								
11. CONTROLLING OFFICE NAME AND ADDRESS U.S. Army Cold Regions Research and Engineering Laboratory Hanover, New Hampshire 03755-1290		12. REPORT DATE December 1985								
14. MONITORING AGENCY NAME & ADDRESS (if different from Controlling Office)		13. NUMBER OF PAGES 53								
		15. SECURITY CLASS. (of this report) Unclassified								
16. DISTRIBUTION STATEMENT (of this Report) Approved for public release; distribution unlimited.										
17. DISTRIBUTION STATEMENT (of the abstract entered in Block 20, if different from Report)										
18. SUPPLEMENTARY NOTES										
19. KEY WORDS (Continue on reverse side if necessary and identify by block number) <table border="0"> <tr> <td>Floe size</td> <td>Ice properties</td> </tr> <tr> <td>Friction factor</td> <td>Laboratory tests</td> </tr> <tr> <td>Ice breaking</td> <td>Model ice</td> </tr> <tr> <td>Ice forces</td> <td>Probability distributions</td> </tr> </table>			Floe size	Ice properties	Friction factor	Laboratory tests	Ice breaking	Model ice	Ice forces	Probability distributions
Floe size	Ice properties									
Friction factor	Laboratory tests									
Ice breaking	Model ice									
Ice forces	Probability distributions									
20. ABSTRACT (Continue on reverse side if necessary and identify by block number) <p>Tests in level ice on an idealized icebreaker bow in the shape of a simple wedge were conducted in the test basin. The horizontal and vertical forces on the wedge were measured, and floe size distribution in the wake of the wedge was observed. From the force measurements, the ice wedge/hull friction factor was calculated and found to be in general agreement with the friction factor measured in separate friction tests. The ice floe length and ice floe area measured in the current study were found to follow log-normal probability distributions defined by the length average L and area average A and corresponding standard deviations S_L and S_A. The results of these tests and other tests conducted at</p>										

DD FORM 1 JAN 73 1473

EDITION OF 1 NOV 65 IS OBSOLETE

Unclassified

SECURITY CLASSIFICATION OF THIS PAGE (When Data Entered)

20. Abstract (cont'd).

another facility showed that the ratios A/h^2 and L/h (A = average floe area, L = average floe length, h = ice thickness) were, for the same type of model ice, directly proportional to the parameter $\sigma/\gamma h$ (σ = ice bending strength, γ = specific weight of water) and $\sigma/\gamma h$, respectively, and independent of the velocity and ice strain modulus or ice characteristic length. However, the coefficients of proportionality appear to depend upon the type of model ice used in the tests. The ratios S_1/A were independent of $\sigma/\gamma h$ but varied with the bow shape and the type of ice. The available field data are not sufficient for meaningful comparison with the laboratory results.

PREFACE

This report was prepared by Dr. Jean-Claude Tatinclaux, Research Hydraulic Engineer, of the Ice Engineering Research Branch, Experimental Engineering Division, U.S. Army Cold Regions Research and Engineering Laboratory. This study was an in-house laboratory independent research.

This report was technically reviewed by Steve Daly and John Rand.

The author wishes to thank Anthony Lozeau and Stephen DenHartog for their help in the conduct of the experiments and Sharon Borland and Leslie Wardwell, who partially analyzed the data.

The contents of this report are not to be used for advertising or promotional purposes. Citation of brand names does not constitute an official endorsement or approval of the use of such commercial products.

Accession	
NTIS	CLASS
DTIC	FORM
Un	CLASS
Dist	
A-1	



CONTENTS

	Page
Abstract	i
Preface	ii
Introduction	1
Experimental set-up and conditions	1
Results of wedge resistance measurements	3
Results of floe size measurements	7
Statistical analysis of data	12
Comparison between model and full-scale data	13
Conclusions and recommendations	14
Literature cited	14
Appendix A: Wedge tests—floe size measurements	15
Appendix B: Wedge tests—histograms of floe length and floe area	31
Appendix C: Cumulative frequency distributions for floe length and floe area	39

ILLUSTRATIONS

Figure

1. Sketch and particulars of experimental wedge	2
2. Views of wedge model and reference frame mounted on towing carriage	2
3. Plot of adimensional resistance versus Froude number	5
4. Definition sketch for the determination of N and T from measured F_x and F_z ..	5
5. Examples of break patterns	7
6. Graphical representation of results	12
7. Relative standard deviations	13
8. Average and range of relative standard deviations	13

TABLES

Table

1. General conditions of tests	4
2. Results of force measurements on wedge	4
3. Calculated friction coefficient between ice and wedge hull	6
4. Results of floe size measurements	8
5. Summary of floe size observation	9
6. Dimensionless laboratory data	10
7. Dimensionless full-scale data	11
8. Correlation matrices for laboratory data	11
9. Relative standard deviations of floe length and floe area	13

LEVEL ICE BREAKING BY A SIMPLE WEDGE

Jean-Claude Tatinclaux

INTRODUCTION

In modeling a ship moving through level ice, it is customary to apply the Froude scaling law. If λ is the geometric scale of the ship model, the thickness h and flexural strength σ of the model ice are scaled in the same ratio from the full-scale values, while the ratio of full-scale to model ship velocity is $\sqrt{\lambda}$. The ice strain modulus E should also be scaled by λ , or the ratio E/σ should be the same at full and model scales, but no existing model ice, saline ice, urea-doped ice, or synthetic ice has been able to achieve this latter requirement; while full-scale values of E/σ are of the order of 5000, the values of E/σ for model ice may vary from as low as 500 to 2000 or more.

Experience has shown that the resistance of ships in level ice is usually predicted satisfactorily by model tests, but that the power requirements predicted from model propulsion tests are usually significantly greater than those observed during full-scale trials. It has been conjectured (Keinonen 1983) that the relatively greater power required at the model scale corresponds to excessive ingestion of ice into the model propeller(s) as compared to actual ice propeller interaction at full scale. Keinonen (1983) further attributed such differences in ice propeller interaction to differences in breaking pattern and broken floe sizes:

In the model tests, the ice is broken into large cusps, the typical size or ice blocks anywhere between 3–6 times the ice thickness. In full scale, the typical blocks are radically smaller being in the range of 0.5–2 times the ice thickness. This is not only due to what is called the breaking pattern for breaking initial ice cusps, which can be scaled reasonably well based on existing experiences, but is probably mainly due to the fact that natural ice is so brittle that it contains dense cracks which have propagated during local ice edge crushing. Conse-

quently, the original cusps fall apart when being pushed down. Model ice cusps tend not to contain such internal cracks. Two things follow: the ice flow around the hull changes due to block size changes and also any ice that may enter the nozzle appears in smaller blocks in full scale causing lesser disturbances in propulsion.

The Ice Committee of the American Towing Tank Conference recommended that basic investigation of the breaking pattern in model ice by ice-breaker models be initiated. One such investigation was recently conducted for the Canadian Coast Guard at the facility of ARCTEC Canada Ltd. (Anonymous 1984) with a model of the ice-breaker MV *Kigoriak* in urea-doped ice and in synthetic model ice. The present study was made in the ice towing basin of the U.S. Army Cold Regions Research and Engineering Laboratory (CRREL) using a simple wedge-shaped bow in urea-doped ice. Full-scale data on ice piece sizes are scarce. The ARCTEC study does contain some data on floe length and area measured during trials of the MV *Kigoriak* and the CCGC *Pierre Radisson*. Another set of floe sizes measured during trials of the USCGC *Katmai Bay* was reported by McKindra and Lutton (1981).

EXPERIMENTAL SET-UP AND CONDITIONS

A simple wedge was selected as an idealized ice-breaker bow for the experiments. The stem and flare angles of the wedge are typical of a conventional icebreaker bow. Sketches and particulars of the wedge are shown in Figure 1. The wedge was rigidly connected to the towing carriage so that it could roll but was prevented from heaving and pitching.

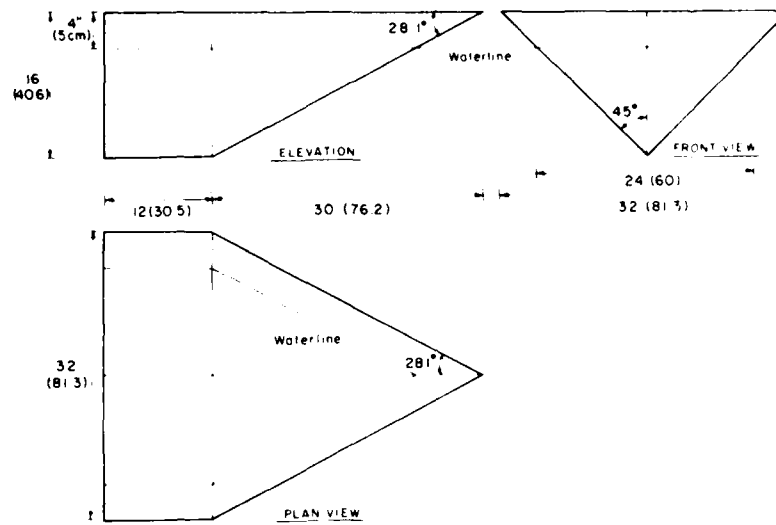
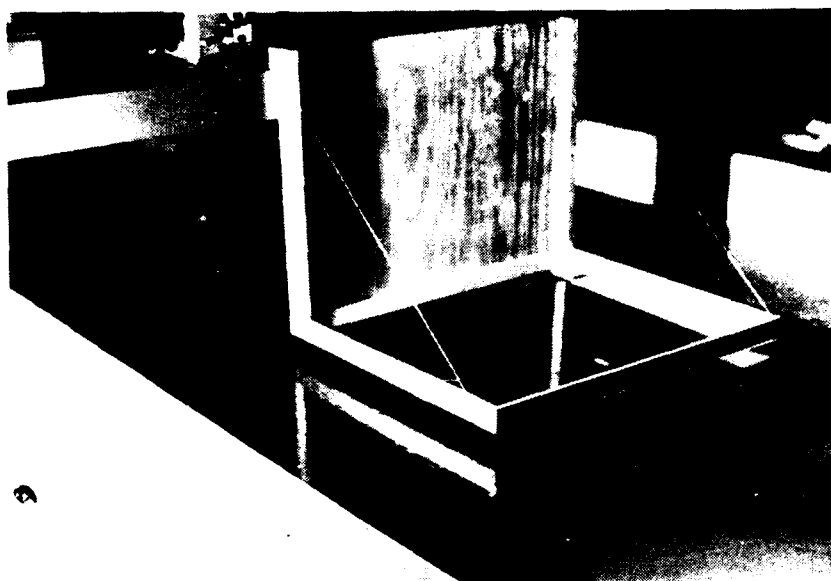


Figure 1. Sketch and particulars of experimental wedge.



a. Wedge and force transducers mounted on towing carriage.

Figure 2. Views of wedge model and reference frame mounted on towing carriage.



b. Frame for floe size measurements.

Figure 2 (cont'd).

A plexiglass sheet marked with orthogonal lines at 10 cm intervals was suspended behind the wedge, a few centimeters above the ice. A still camera mounted above the plexiglass sheet photographed the broken ice floes in the wake of the wedge during each test. These pictures were used to measure the floe sizes. In addition to floe size, the forces exerted on the wedge both in the direction of motion, F_x , and in the upward vertical direction, F_z , were measured during each test. Views of the experimental set-up are shown in Figure 2.

Tests were made in nine level ice sheets of various thickness h , bending strength σ , and strain modulus E . The ice sheets were grown from a water bath with a 0.9% concentration by weight of urea. The ice sheets were initiated by the wet seeding method at an air temperature of -7 to -10°C and grown at an air temperature of -15 to -20°C . The resulting ice has a columnar structure closely resembling that of first-year sea ice (Gow 1984). The ice thickness was measured by a caliper with an accuracy of 1 mm, the bending strength was obtained from in-situ small cantilever beam tests, and the ice characteristic length l , and corresponding strain modulus E were calculated from the measurement of the ice sheet deflection due to a localized load. In addition, the kinetic friction

coefficient μ between the ice and the wedge was determined by measuring the force T required to pull a loaded ice sample, with a total normal load N , over the wedge surface set horizontally. This friction coefficient, $\mu = T/N$, was measured for both the top and the bottom surfaces of the ice with the results

$$\begin{aligned} \text{top of ice: } \mu &= 0.054 \pm 0.011 \\ \text{bottom of ice: } \mu &= 0.033 \pm 0.002 \end{aligned}$$

In each ice sheet, three or four tests were made at constant speed V from 7.5 to 45 cm/s. A total of 30 tests were made; the conditions are listed in Table 1.

Results of wedge resistance measurements

The measured forces F_x and F_z are listed in Table 2. Their normalized forms $X = F_x/\gamma B h^2$, $Z = F_z/\gamma B h^2$, where B is the maximum wedge beam at the water line, are plotted against the Froude number, $F_n = V/\sqrt{g h}$, in Figure 3 with the nondimensional ice strength, $C_n = \sigma/\gamma h$, as a parameter. It can be seen that both X and Z increase linearly with F_n , but that no systematic variation with C_n is apparent.

Table 1. General conditions of tests.

Ice sheet no.	Test no.	Ice thickness, h (cm)	Ice strength, σ (kPa)	Ice Young's modulus, E (MPa)	Ice characteristic length, l_c (cm)	Velocity, V (cm/s)
1	1	3.3	66.0	71	39.3	14.9
	2	3.3	66.0	71	39.3	30.1
	3	3.3	66.0	71	39.3	45.3
2	4	3.1	34.0	49	34.2	15.0
	5	3.1	34.0	49	34.2	30.0
	6	3.1	34.0	49	34.2	45.2
3	7	5.0	37.0	60	51.4	45.2
	8	5.0	37.0	60	51.4	30.1
	9	5.0	37.0	60	51.4	14.9
4	10	3.6	33.0	46	37.6	45.3
	11	3.6	33.0	46	37.6	30.3
	12	3.6	33.0	46	37.6	15.2
5	13	5.4	50.0	96	61.3	45.2
	14	5.4	50.0	96	61.3	30.0
	15	5.4	50.0	96	61.3	14.9
6	16	1.85	40.7	48	23.1	45.2
	17	1.85	40.7	48	23.1	30.0
	18	1.85	40.7	48	23.1	14.9
7	19	6.0	49.0	251	84.3	45.2
	20	6.0	49.0	251	84.3	30.2
	21	6.0	49.0	251	84.3	14.9
	22	6.0	40.0	251	84.3	7.2
8	23	6.0	47.0	100	67.0	45.0
	24	6.0	47.0	100	67.0	29.9
	25	6.0	47.0	100	67.0	14.8
	26	6.0	47.0	100	67.0	7.6
9	27	4.0	44.0	38	38.8	45.1
	28	4.0	44.0	38	38.8	30.0
	29	4.0	44.0	38	38.8	14.9
	30	4.0	44.0	38	38.8	7.6

Table 2. Results of force measurements on wedge.

Test no.	$F_N = (V/\sqrt{gh})$	$C_N = (\sigma/\gamma h)$	F_x (N)	F_z (N)	$F_x/\gamma Bh^3$	$F_z/\gamma Bh^3$	$F_N \cdot C_N$
1	0.26	204	34.8	49.6	5.34	7.62	53
2	0.53	204	44.5	67.2	6.83	10.32	108
3	0.80	204	48.7	71.9	7.48	11.04	163
4	0.27	112	28.6	44.8	4.98	7.80	30
5	0.54	112	39.2	68.3	6.82	11.88	60
6	0.82	112	45.0	70.5	7.83	12.27	92
7	0.65	75	93.6	131.8	6.26	8.82	49
8	0.43	75	96.5	131.7	6.45	8.81	32
9	0.21	75	66.7	119.2	4.46	7.97	16
10	0.77	95	57.6	93.5	7.43	12.06	73
11	0.51	95	48.7	71.7	6.28	9.25	48
12	0.26	95	40.3	52.1	5.20	6.72	25
13	0.62	94	164.0	248.6	9.40	14.26	58
14	0.41	94	141.1	202.8	8.09	11.63	39
15	0.20	94	106.7	147.2	6.12	8.44	19
16	1.06	224	26.6	53.9	13.00	26.33	237
17	0.70	224	20.8	31.5	10.16	15.39	157
18	0.35	224	16.6	19.9	8.11	9.72	78
19	0.59	83	202.0	299.8	9.38	13.93	49
20	0.39	83	165.6	225.4	7.69	10.47	32
21	0.19	83	147.5	180.6	6.85	8.39	16
22	0.09	83	136.4	187.0	6.34	8.69	7.5
23	0.59	80	162.6	230.5	7.55	10.71	47
24	0.39	80	160.1	225.5	7.44	10.47	31
25	0.19	80	135.6	189.4	6.30	8.80	15
26	0.10	80	125.0	164.4	5.81	7.64	8
27	0.72	112	61.0	101.2	6.38	10.58	81
28	0.48	112	51.6	69.6	5.39	7.27	54
29	0.24	112	43.3	58.8	4.53	6.15	27
30	0.12	112	36.2	47.5	3.78	4.96	13

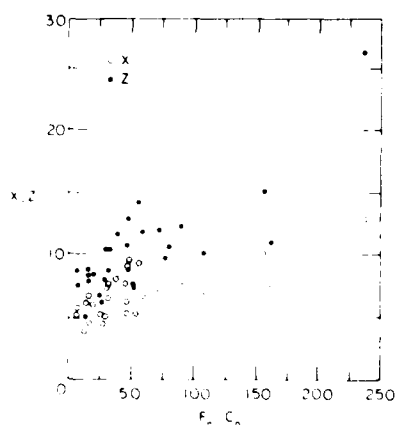
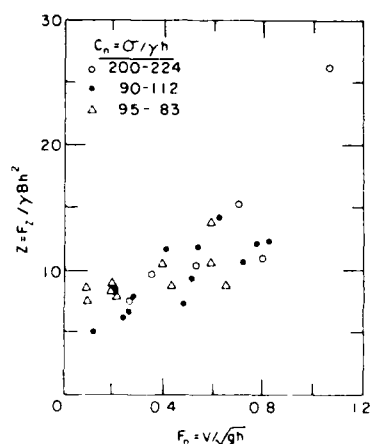
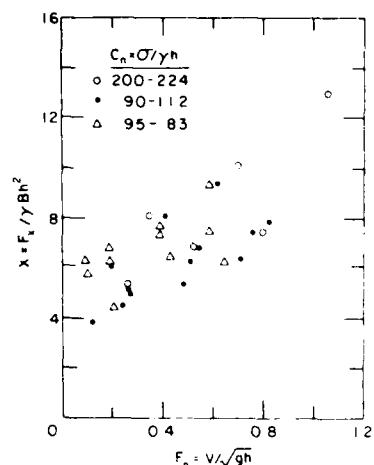


Figure 3. Plot of adimensional resistance versus Froude number.

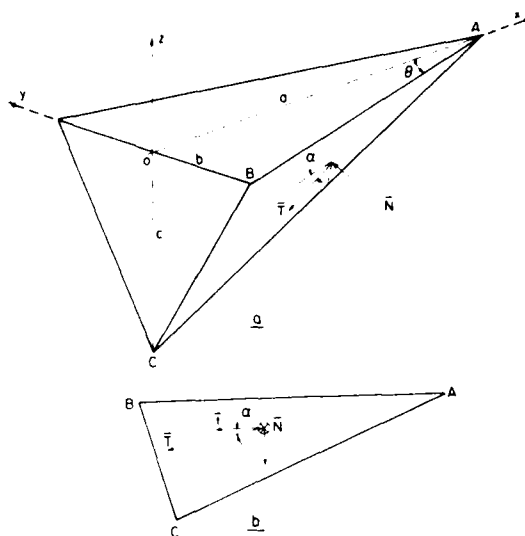


Figure 4. Definition sketch for the determination of N and T from measured F_x and F_z .

From the measured forces F_x and F_z , it is possible to estimate the overall normal and tangential forces, N and T , exerted on each face of the wedge. The exact determination of N and T would have required that the transverse force F_y in the horizontal plane acting on one face of the wedge be measured. Nevertheless, even with F_y lacking, and since the wedge hull has no vertical part, a range of values of N and T can be determined from which a range of the friction coefficient $\mu = T/N$ can be calculated. Let ABC be the plane of one face of the wedge defined by the three points $A(a,0,0)$, $B(0,b,0)$, and $C(0,0,c)$ in the Cartesian frame of reference $OXYZ$ shown in Figure 4. The OXY plane coincides with the horizontal plane, with axis OX along the wedge centerline and axis OY in the transverse direction. Axis OZ is vertical upward to complete the system of axes. The unit vector \mathbf{n} normal to the plane ABC and directed toward the inside of the wedge has the components

$$\begin{aligned} n_1 &= -\frac{bc}{\Delta} \\ n_2 &= \frac{ac}{\Delta} \\ n_3 &= \frac{ab}{\Delta} \end{aligned} \quad (1)$$

with $\Delta = (a^2b^2 + b^2c^2 + c^2a^2)^{1/2}$. In the plane ABC, two unit vectors, \mathbf{t} and \mathbf{s} , are defined such that \mathbf{t} is in a horizontal plane and \mathbf{s} forms with \mathbf{n} and \mathbf{t} a right-handed system. The components of \mathbf{t} and \mathbf{s} in OXYZ are

$$\begin{aligned} t_1 &= -\frac{a}{\sqrt{a^2+b^2}} \\ t_2 &= -\frac{b}{\sqrt{a^2+b^2}} \\ t_3 &= 0 \end{aligned} \quad (2)$$

$$\begin{aligned} s_1 &= -\frac{ab^2}{\Delta\sqrt{a^2+b^2}} \\ s_2 &= \frac{a^2b}{\Delta\sqrt{a^2+b^2}} \\ s_3 &= -\frac{c(a^2+b^2)}{\Delta\sqrt{a^2+b^2}} \end{aligned} \quad (3)$$

The normal force $\mathbf{N} = N\mathbf{n}$ acting on ABC has the components (Nn_1, Nn_2, Nn_3) , while the tangential force \mathbf{T} is defined by

$$\mathbf{T} = T\cos\alpha\mathbf{t} + T\sin\alpha\mathbf{s} \quad (4)$$

where α is the angle between \mathbf{T} and \mathbf{t} .

The magnitudes F_x and F_z of the total forces acting on the wedge in the X - and Z -directions are then

$$F_x = |2Nn_1 + 2T\cos\alpha t_1 + 2T\sin\alpha s_1| \quad (5a)$$

$$F_z = |2Nn_3 + 2T\cos\alpha t_3 + 2T\sin\alpha s_3| \quad (5b)$$

that is,

$$F_x = 2N\frac{bc}{\Delta} + \frac{2aT}{\Delta\sqrt{a^2+b^2}} (\Delta\cos\alpha + b^2\sin\alpha) \quad (6a)$$

$$F_z = 2N\frac{ab}{\Delta} - \frac{2cT\sqrt{a^2+b^2}\sin\alpha}{\Delta} \quad (6b)$$

In the case of the present wedge, where $b = c$, the calculated overall friction factor $\mu_c = T/N$ is given by

$$\mu_c =$$

$$\frac{[R - (b/a)]\sqrt{1 + (b^2/a^2)}}{R[1 + (b^2/a^2)]\sin\alpha + (b/a)\sin\alpha + \sqrt{2 + (b^2/a^2)}\cos\alpha} \quad (7)$$

with $R = F_z/F_x$. It is easily shown that μ_c first decreases with increasing α , reaches a minimum μ_m at $\alpha = \alpha_m$ given by

$$\tan\alpha_m = \frac{R[1 + (b^2/a^2)] + (b/a)}{\sqrt{2 + (b^2/a^2)}} \quad (8)$$

and then increases as α increases further.

The calculated values of μ_0 (i.e. μ_c at $\alpha = 0$), α_m , and μ_m for each of the tests are presented in Table 3. The angle α_m is seen to remain nearly constant,

Table 3. Calculated friction coefficient between ice and wedge hull.

Test no.	$R = F_z/F_x$	μ_0	α_m	μ_m
1	0.702	0.126	43.5	0.092
2	0.662	0.097	42.5	0.071
3	0.677	0.108	42.9	0.079
4	0.638	0.079	41.8	0.059
5	0.574	0.030	40.0	0.023
6	0.638	0.079	41.8	0.059
7	0.710	0.133	43.7	0.096
8	0.733	0.150	44.3	0.107
9	0.560	0.020	39.6	0.015
10	0.616	0.062	41.2	0.047
11	0.679	0.109	42.9	0.080
12	0.774	0.180	45.3	0.127
13	0.660	0.095	42.4	0.070
14	0.696	0.122	43.3	0.089
15	0.725	0.144	44.1	0.103
16	0.494	-0.030	37.7	-0.023
17	0.660	0.095	42.4	0.070
18	0.834	0.226	46.7	0.155
19	0.674	0.105	42.8	0.077
20	0.735	0.151	44.3	0.108
21	0.817	0.213	46.3	0.147
22	0.729	0.147	44.2	0.106
23	0.705	0.129	43.6	0.094
24	0.710	0.132	43.7	0.096
25	0.716	0.137	43.9	0.099
26	0.760	0.170	45.0	0.121
27	0.603	0.052	40.9	0.040
28	0.741	0.156	44.5	0.111
29	0.736	0.152	44.4	0.109
30	0.762	0.172	45.0	0.121
Averages:		0.118	43.2	0.085
Standard deviations:		0.055	2.0	0.038

varying within the narrow range of 40–45°, and μ_c decreases by about 30% between $\alpha = 0$ and $\alpha = \alpha_m$. The average value of μ_m is found to be 44% larger than the friction factor measured in the friction tests between the top of the ice samples and the wedge surface. However, the range of calculated values of μ_m overlaps that of the measured values of μ . It should be pointed out that since μ_c is practically proportional to $(R = a/b)$, a relatively small error in R , that is in F_c or F_c or both, may result in a significantly larger error in μ_c . In addition, the larger measured values of μ_c are obtained with the top of the ice sample on the wedge surface while, during icebreaking tests, the edges of the broken ice floes may also rub against the wedge with a possibly higher friction coefficient. Therefore, even though the calculated values of μ are on the average larger than the measured ones, the two sets of values are not inconsistent with each other, which validates the experimental technique used for estimating the friction coefficient between the ice and the hull of a model ship or other structure.

Results of floe size measurements

Examples of the break patterns ahead of and behind the wedge are shown in Figure 5. From the photographs taken through the grid (Fig. 5b), the

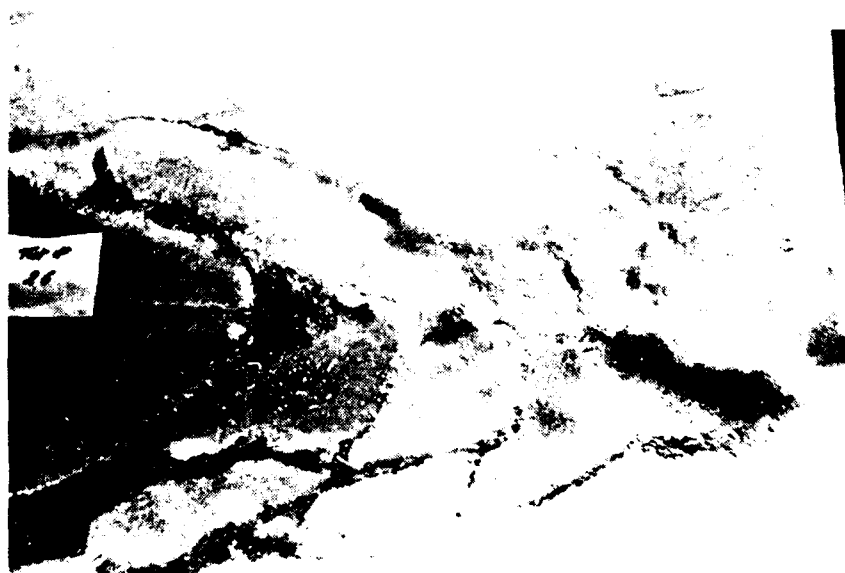
major dimensions, length L and width W , of the broken floes in the wake of the wedge were measured and their areas A were calculated depending upon the shape of each floe, which was approximated by one of seven simple geometric shapes. The results of these measurements are listed for each test in the tables of Appendix A. They are summarized in Table 4 as the overall average area A and length L of the floes for each test and the corresponding standard deviations.

The four variables that may affect floe size distribution characteristics are ice thickness h , ice strength σ , ice characteristic length l_c , and velocity V . Visual inspection of the results obtained for each series of tests made in an ice sheet where only the velocity was varied shows no systematic variation of A and L or their standard deviations with V . It is then assumed that A and L are functions of h , σ , and l_c only, or in dimensionless form that

$$\frac{A}{l_c^2} , \frac{L}{l_c} = f \left[\frac{l_c}{h} , \frac{\sigma}{\gamma l_c} \right] \quad (9a)$$

or

$$\frac{A}{h^2} , \frac{L}{h} = f \left[\frac{l_c}{h} , \frac{\sigma}{\gamma h} \right] \quad (9b)$$



a. Ahead of wedge.

Figure 5. Examples of break patterns.



b. In wake of wedge.

Figure 5 (cont'd). Examples of break patterns.

Table 4. Results of floe size measurements.

Test no.	No. of ice pieces	Floe area (cm ²)		Floe length (cm)		Ice sheet no.
		Average A	Std. dev. S _A	Average L	Std. dev. S _L	
4	26	144	106	19.3	7.2	2
5	16	165	89	25.3	7.3	
6	24	120	93	20.0	8.7	
7	23	200	127	22.9	10.8	3
8	23	178	92	22.0	6.6	
9	28	221	222	24.9	13.8	
10	37	176	123	23.6	9.8	4
11	35	143	106	23.5	13.0	
12	19	125	96	19.3	9.4	
13	31	189	120	25.9	10.1	5
14	21	139	112	20.5	9.5	
15	29	151	115	19.0	8.6	
16	60	68	78	11.9	7.4	6
17	35	123	74	18.4	6.4	
18	34	121	77	17.2	6.0	
19	21	279	200	30.6	14.0	7
20	16	354	182	34.3	12.3	
22	16	400	382	35.8	20.6	
23	19	271	256	27.0	14.0	8
24	18	271	160	30.3	8.9	
25	23	210	125	25.2	11.2	
26	20	155	77	22.3	7.3	9
27	22	256	160	32.3	12.6	
28	17	207	136	28.8	11.2	
29	16	182	89	29.1	8.9	
30	19	233	110	29.7	8.3	

Table 5. Summary of floe size observation.

a. Laboratory data.

Test no.	h (cm)	σ (kPa)	l_c (cm)	Floe area		Floe length		No. of ice pieces
				A (cm ²)	s.d. (cm ²)	L (cm)	s.d. (cm)	
Wedge in urea ice								
4-5-6	3.1	34.0	34.2	140	97	21.0	8.1	66
7-8-9	5.0	37.0	51.4	200	161	23.4	11.0	74
10-11-12	3.6	33.0	37.6	153	112	22.7	11.1	91
13-14-15	5.4	50.0	61.3	162	116	22.0	9.8	81
16-17-18	1.9	40.7	23.1	97	81	15.0	7.4	129
19-20-22	6.0	49.0	84.3	341	263	33.3	15.7	53
23-24-25-26	6.0	47.0	67.0	224	170	26.1	10.8	80
27-28-29-30	4.0	44.0	38.8	223	129	30.1	10.4	74
Kigoriak model in urea ice								
1-2-3	6.7	47.0	102.6	242	186	27.2	15.7	79
4-5-6	7.0	54.0	84.6	286	264	34.6	22.0	63
7-8-9	2.9	122.0	52.6	154	162	21.6	15.4	88
10-11-12	2.4	85.0	38.8	221	273	25.6	18.4	48
13-14-15	3.0	59.0	35.6	138	145	21.2	13.5	105
16-17-18	2.9	51.0	28.0	163	157	22.2	12.9	71
Kigoriak model in synthetic ice								
1-2-3-4	5.65	142.0	84.7	316	530	20.3	16.6	145
5-6-7-8	3.05	115.0	50.3	185	243	16.8	12.7	166
9-10	5.6	115.0	79.3	335	498	22.7	16.8	58
11-12	4.7	115.0	69.6	170	262	16.1	15.0	91

b. Full-scale data.

Run no.	σ (kPa)	h (m)	Floe area		Floe length		No. of ice pieces
			A (m ²)	S _A (m ²)	L (m)	S _L (m)	
MV Kigoriak							
1	—	N.A.	1.81	2.81	1.49	0.99	41
2	—	N.A.	0.43	0.38	0.96	0.38	32
3	—	N.A.	1.84	1.22	1.73	0.71	27
4	—	N.A.	2.11	1.82	1.98	0.97	41
5	—	N.A.	2.30	2.15	1.76	0.61	19
6	—	N.A.	4.37	2.98	2.98	1.09	29
Pierre Radisson							
1	—	1.07	7.9	11.7	3.80	3.63	11
2	—	0.98	3.7	3.7	2.63	2.22	14
3	—	1.05	5.2	9.4	2.27	2.74	25
4	—	1.05	20.9	19.4	5.21	3.41	10
Katmai Bay							
1100	660	0.36	—	—	10.4	1.1	54
1110	660	0.37	—	—	7.9	3.6	85
1120	650	0.36	—	—	9.4	5.3	91
1130	650	0.38	—	—	8.0	3.7	61
1200	620	0.36	—	—	9.6	6.3	52
1210	620	0.33	—	—	9.2	3.6	36
1220	620	0.28	—	—	8.9	5.0	65
1300	640	0.38	—	—	9.8	4.9	54
1310	640	0.41	—	—	7.7	4.2	36
1320	640	0.42	—	—	7.9	4.7	35
1330	640	0.41	—	—	8.6	3.4	24

Table 6. Dimensionless laboratory data.

Ice sheet no.	l_c/h	$\sigma/\gamma l_c$	$\sigma/\gamma h$	A/l_c^2	L/l_c	A/h^2	L/h	S_L/L	S_A/A
Wedge in ice									
2	11.0	10.1	112	0.120	0.61	14.6	6.77	0.39	0.69
3	10.3	7.3	75	0.076	0.46	8.0	4.68	0.47	0.81
4	10.4	9.0	93	0.108	0.60	11.8	6.31	0.49	0.73
5	11.4	8.3	94	0.043	0.36	5.5	4.07	0.45	0.72
6	12.5	18.0	224	0.182	0.65	28.4	8.11	0.49	0.84
7	14.1	5.9	83	0.048	0.40	9.5	5.55	0.47	0.77
8	11.2	7.2	80	0.050	0.39	6.2	4.34	0.41	0.76
9	9.7	11.6	112	0.148	0.78	13.9	7.54	0.35	0.58
Kigoriak in urea ice									
1	15.3	4.6	70	0.023	0.27	5.4	4.06	0.58	0.77
2	12.1	6.5	79	0.040	0.41	5.9	4.94	0.64	0.92
3	18.1	23.6	428	0.056	0.41	18.3	7.45	0.71	1.05
4	16.2	22.3	361	0.147	0.66	38.3	10.67	0.72	1.24
5	11.9	16.9	201	0.109	0.60	15.3	7.07	0.64	1.05
6	9.7	18.6	180	0.208	0.79	19.4	7.66	0.58	0.96
Kigoriak in synthetic ice									
1	15.0	17.1	255	0.044	0.24	9.9	3.59	0.82	1.68
2	16.5	23.6	384	0.073	0.33	19.9	5.51	0.76	1.31
3	14.2	14.8	209	0.053	0.29	10.7	4.05	0.74	1.49
4	14.8	18.3	249	0.035	0.23	7.7	3.43	0.93	1.54

The relationships represented by eq 9a and 9b are in principle equivalent, but the second form may provide a better means of comparing laboratory data and available field measurements for which the ice characteristic length is seldom measured.

The average data for each ice sheet have been collected in Table 5, which also lists the laboratory and field data reported in the study mentioned earlier (McKindra and Lutton 1981, Anonymous 1984). Known laboratory data in dimensionless form are listed in Table 6, dimensionless full-scale data in Table 7.

1. Analytical considerations

The authors of the study by ARCTEC Canada Ltd. (Anonymous 1984) state that, according to the elastic theory of semi-infinite beams and plates on elastic foundation, the length of the broken ice pieces should be proportional to l_c and thus the ratios L/l_c and A/l_c^2 should be relatively constant with respect to any other parameter. However, this relationship is valid, at least for a semi-infinite floating beam subjected to a downward load at its free end, only as long as the beam breaks before its free end becomes submerged, which was shown (Yean et al. 1981) to be the case only for

$$E/\sigma > C_1(\sigma/\gamma h) \quad (10)$$

with C_1 approximately equal to 400. Yean et al. (1981) also showed that there is another extreme for E/σ , namely

$$E/\sigma < C_2(\sigma/\gamma h) \quad (11)$$

with C_2 approximately equal to 40, beyond which the ratio of broken beam length to ice thickness L/h is proportional to $(\sigma/\gamma h)^{1/2}$ and independent of the ice strain modulus E and thus of the ice characteristic length l_c . By analogy it can be assumed that for a semi-infinite plate, the ratio between broken pieces area and h^2 is proportional to $\sigma/\gamma h$ when the relation (11) is satisfied (with a yet undetermined value of C_2).

2. Presentation of experimental results

The correlation matrices for the dimensionless laboratory and full-scale data in Table 6 and 7 are given in Table 8. From Table 8, it is apparent that there is no correlation between A/l_c^2 , A/h^2 , L/l_c , or L/h and l_c/h . As has been observed previously (Sodhi et al. 1983), the ratio l_c/h , both for laboratory model ice and natural ice, varies between 10 and 15, approximately. This range of variation may appear fairly narrow, but it should be kept in mind that, for constant $\sigma/\gamma h$, a common modeling parameter, a 50% increase in l_c/h corresponds to a five-fold increase in E/σ .

Table 7. Dimensionless full-scale data.

Run no.	$\sigma/\gamma h$	A/h^2	L/h	S_A/A	S_L/L
Kigoriak					
1				1.55	0.66
2				0.88	0.40
3				0.66	0.41
4				0.86	0.49
5				0.93	0.35
6				0.68	0.37
Pierre Radisson					
1		6.90	3.55	1.48	0.96
2		3.85	2.68	1.00	0.84
3		4.72	2.16	1.81	1.21
4		18.96	4.96	0.93	0.65
Katmai Bay					
1100	187		28.9		0.11
1110	182		21.4		0.46
1120	184		26.1		0.56
1130	174		21.1		0.46
1200	166		25.3		0.66
1210	192		27.9		0.39
1220	226		31.8		0.56
1300	172		25.8		0.50
1310	159		18.8		0.55
1320	155		18.8		0.59
1330	159		21.0		0.40

Table 8. Correlation matrices for laboratory data.

	Wedge in urea ice			Kigoriak in urea ice*			Kigoriak in synthetic ice			Wedge tests, Kigoriak in urea ice		
	l_c/h	$\sigma/\gamma l_c$	$\sigma/\gamma h$	l_c/h	$\sigma/\gamma l_c$	$\sigma/\gamma h$	l_c/h	$\sigma/\gamma l_c$	$\sigma/\gamma h$	l_c/h	$\sigma/\gamma l_c$	$\sigma/\gamma h$
A/l_c^2	0.225	0.901	0.804	0.460	0.879	0.647	0.723	0.648	0.762	0.278	0.842	0.648
A/h^2	0.179	0.939	0.953	0.318	0.897	0.983	0.869	0.812	0.897	0.339	0.909	0.954
L/l_c	0.438	0.674	0.510	0.460	0.907	0.677	0.650	0.607	0.704	0.387	0.761	0.559
L/h	0.025	0.804	0.744	0.167	0.952	0.982	0.816	0.777	0.856	0.192	0.902	0.897

* Tests for sheet 3 for Kigoriak in urea ice deleted.

The results in Table 8 also show that the highest correlation for the laboratory data exists between A/h^2 or L/h and $\sigma/\gamma h$. Graphical representation of the data are given in Figure 6a as A/h^2 versus $\sigma/\gamma h$ and in Figure 6b as L/h versus $\sigma/\gamma h$.

From Figures 6a and 6b it is apparent that

1. There is indeed a linear relationship between A/h^2 and $\sigma/\gamma h$, while L/h can be considered to vary as $(\sigma/\gamma h)^{1/2}$.
2. Tests run in urea ice both with the wedge (current study) and the model of the Kigoriak give similar results. This would indicate that

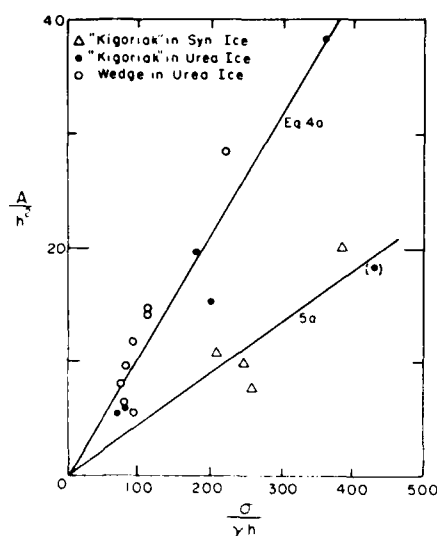
the bow shape—a sharp edge for the wedge, a spoon shape for the Kigoriak—has little or no influence on the size of the broken ice floes.

3. Tests run in synthetic ice give significantly smaller ice pieces.

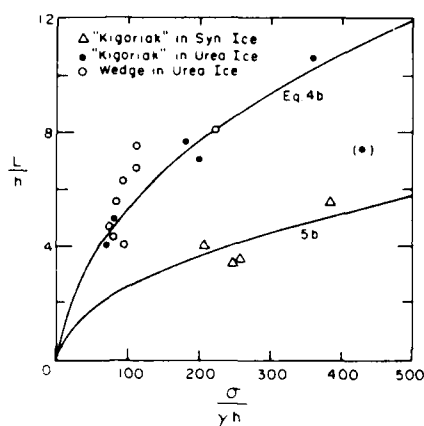
Linear regression analysis of the data led to the following equations. For urea ice:

$$(A/h^2) = 0.105(\sigma/\gamma h) \quad (12a)$$

$$(L/h) = 0.540(\sigma/\gamma h)^{1/2} \quad (12b)$$



a. A/h^2 versus $\sigma/\gamma h$.



b. L/h versus $\sigma/\gamma h$.

Figure 6. Graphical representation of results.

For synthetic ice:

$$(A/h^2) = 0.045(\sigma/\gamma h) \quad (13a)$$

$$(L/h) = 0.259(\sigma/\gamma h)^{1/2}. \quad (13b)$$

Statistical analysis of data

McKindra and Lutton (1981) found that the length of the ice floes broken by the USCGC *Katmai Bay* during the 1979 trials in the St. Mary's River and Whitefish Bay followed a log normal probability distribution.

The probability density function for the log-normal random variable X is

$$f(X) = \frac{1}{\sqrt{2\pi} b X} \exp\left[-\frac{(\ln X - a)^2}{2b^2}\right] \quad (14)$$

and the cumulative frequency distribution is given by

$$P(X_0) = \text{prob}(X \leq X_0) = \int_0^{X_0} f(X) dX. \quad (15)$$

In eq 14 the parameters a and b are related to the mean M and standard deviation S of the random variable X by

$$a = \ln \frac{M^2}{\sqrt{M^2 + S^2}} \quad (16)$$

$$b = \left[\ln \frac{M^2 + S^2}{M^2} \right]^{1/2} \quad (17)$$

The non-dimensional floe length and floe area, L/h and A/h^2 , respectively, measured in the current laboratory study were analyzed assuming they followed log-normal distributions.

Histograms of L/h and A/h^2 for each ice sheet tested were obtained as shown in the figures of Appendix B. For each histogram, the offset and cell width (and consequently the number of cells) were determined from the constraint that the largest cell height, i.e. the relative number of observations in that cell, exceeded 20%, and by optimizing the χ^2 -goodness-of-fit to a log-normal distribution. The cumulative frequency distributions are shown in the figures of Appendix C on which the theoretical distributions given by eq 15 for the corresponding mean and standard deviation are overlaid for comparison. It can be seen that the data generally fit a log-normal distribution well, especially in the upper 50% of the data, while some deviation occurs for the lower 50% of the data.

Equations 14 and 15 are totally defined by the mean and standard deviation of the random variable. It has been shown, at least for the laboratory data, that the mean L/h^2 are functions of $\sigma/\gamma h$ (eq 12 and 13). When the corresponding standard deviations S_L/h and S_A/h^2 were plotted against $\sigma/\gamma h$, they also followed similar curves. The ratios S_L/L and S_A/A were then found to be practically constant over the range of variation of $\sigma/\gamma h$, not only

for the current study but also for the other laboratory study and for the full-scale data obtained during the *Katmai Bay* trials, as shown in Figure 7. The average values of S_L/L and S_A/A plus and minus one standard deviation are presented in Figure 8 for all the data sets available.

Comparison between model and full-scale data

The available full-scale data are unfortunately not sufficient for meaningful comparison with the model test results. The data from the MV *Kigoriak* include neither ice thickness nor ice bending

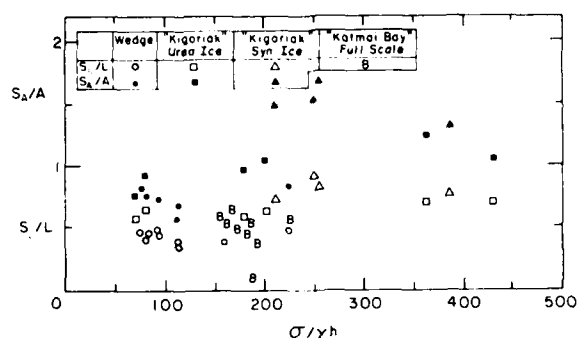


Figure 7. Relative standard deviations, S_L/L and S_A/A , versus $\sigma/\gamma h$.

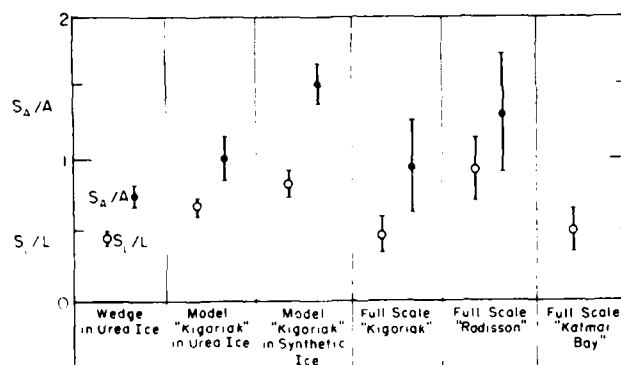


Figure 8. Average and range of relative standard deviations, S_L/L and S_A/A , from all available sources.

Table 9. Relative standard deviations of floe length and floe area.

Vessel and type of test	S_L/L	S_A/A
Wedge in urea ice	0.44 ± 0.05	0.74 ± 0.08
<i>Kigoriak</i> in urea ice	0.65 ± 0.06	1.00 ± 0.16
<i>Kigoriak</i> in synthetic ice	0.81 ± 0.09	1.51 ± 0.15
<i>Kigoriak</i> full-scale	0.45 ± 0.12	0.93 ± 0.32
<i>Radisson</i> full-scale	0.92 ± 0.23	1.31 ± 0.42
<i>Katmai Bay</i> full-scale	0.48 ± 0.15	N.A.

strength, and those for the CCGC *Pierre Radisson* lack ice strength measurements. The data obtained during the *Katmai Bay* trials do contain both ice thickness and ice strength, but their range of variations and, therefore, that of the parameter $\sigma/\gamma h$ are extremely narrow.

The *Katmai Bay* results for L/h are found to be much higher, ranging from 19 to 32, than either those from the model tests, which vary between 6.8 and 10, or those from the *Pierre Radisson* trials, which have a maximum of 5. The ice thickness during the *Katmai Bay* trials in level ice was 30 to 40 cm and the ice bending strength varied between 620 and 660 kPa. McKindra and Lutton (1981) report average length of ice floes of the order of 8 to 10 m with maximums ranging from 17 to 31 m and minimums of 2 to 4 m. In view of the ice thickness and of the icebreaker dimensions (42 m in length and 10.4 m in beam), the ice floe lengths appear excessive. One may wonder whether the unit of the measurements was reported correctly: indeed, if the lengths presented were in feet rather than in meters, then the non-dimensional data for the *Katmai Bay* are in excellent agreement with the laboratory data.

The results of the ratios S_t/L and S_s/A presented in Figure 8 also show significant variation between laboratory and field data as well as from one bow shape to another. However, the range of data and the range of bow shapes investigated are not sufficient to even conjecture as to which parameters, such as L/h , stem angle, flare angle, ship beam over length ratio, etc., the observed variations can be attributed.

CONCLUSIONS AND RECOMMENDATIONS

1. The laboratory tests have shown that the ratios A/h^2 and L/h are proportional to the parameter $\sigma/\gamma h$ raised to the power 1 and $1/2$, respectively, but are independent of the ice strain modulus or characteristic length.

2. The average ice floe size appears to be independent of the shape of the icebreaker bow.

3. The ratios of standard deviation over mean for both floe length and floe area are independent

of $\sigma/\gamma h$ but may vary with some yet-undetermined parameters.

4. The model floe size is affected by the type of model ice used in the experiments. Synthetic ice produces smaller floes than urea-doped ice.

5. Additional laboratory studies on other icebreaker bow shapes are required, and detailed field observation including mechanical properties in addition to ice thickness are needed.

6. If it is found that field and laboratory results are in agreement as far as relative floe size is concerned, other causes for the excessive power requirements predicted by model tests as compared to full-scale observation are to be investigated, e.g. dynamics of propulsion system, and other ice properties such as shear and compression strengths, which may not affect the ice breaking resistance but may influence the ice propeller interaction.

LITERATURE CITED

- Anonymous** (1984) Modeling the broken channel. Canadian Coast Guard, Report TP5373E, Ottawa, Canada.
- Gow, A.** (1984) Crystalline structure of urea ice sheets used in modeling in the CRREL test basin. In *Proceedings, IAHR Ice Symposium 1984, Hamburg, Germany*, vol. II, pp. 241-253.
- Keinonen, A.** (1983) Major scaling problems with ice model testing of ships. *Proceedings, 20th American Towing Tank Conference, Hoboken, New Jersey*, vol. II.
- McKindra, C.D. and T.C. Lutton** (1981) Statistical analysis of broken ice dimensions generated during 140-ft WTGB icebreaker trials. *Proceedings, 6th International Conference, POAC 81, Quebec, Canada*, vol. 1, pp. 235-243.
- Sodhi, D.S., C.R. Martinson and W.B. Tucker, III** (1985) Determining the characteristic length of floating ice sheets by moving loads. For presentation at Offshore Mechanics and Arctic Engineering Symposium, Dallas, Texas.
- Yean, J.S., J.-C. Tatinclaux and A.G. Cook** (1981) Ice forces on two-dimensional sloping structures. Iowa Institute of Hydraulic Research, Iowa City, Iowa, IIHR Report No. 230.

APPENDIX A: WEDGE TESTS—FLOE SIZE MEASUREMENTS

<i>Shape code</i>	<i>Approximate geometric shape of floe</i>
1	Rectangle
2	Triangle
3	Trapezoid
4	Diamond
5	Arc
6	Semi-circle
7	Ellipse

SIMPLE WEDGE TEST - RESULTS OF TEST # 4 - PIECE SIZE

FLOE No.	SHAPE CODE	LENGTH (cm)	WIDTH (cm)	AREA (cm2)
1	4	10.0	3.5	17.5
2	4	11.0	5.5	30.3
3	1	3.5	2.5	8.8
4	4	17.0	6.5	55.3
5	3	16.8	5.5	92.1
6	1	11.5	3.0	34.5
7	2	27.0	15.0	202.5
8	3	12.5	12.5	156.3
9	5	24.0	8.0	192.0
10	1	29.0	13.5	391.5
11	4	31.0	17.5	271.3
12	1	23.0	14.0	322.0
13	2	24.0	8.0	96.0
14	4	23.5	7.5	88.1
15	1	17.0	8.0	136.0
16	4	24.0	8.5	102.0
17	4	20.0	10.5	105.0
18	2	26.0	20.0	260.0
19	4	24.0	10.0	120.0
20	5	20.0	6.5	130.0
21	1	10.0	8.0	80.0
22	1	22.0	2.5	55.0
23	1	24.0	10.5	252.0
24	1	26.5	12.0	318.0
25	2	8.0	7.0	28.0
26	1	16.0	13.0	208.0

SIMPLE WEDGE TEST - RESULTS OF TEST # 5 - PIECE SIZE

FLOE No.	SHAPE CODE	LENGTH (cm)	WIDTH (cm)	AREA (cm2)
1	6	32.5	6.0	133.5
2	1	19.5	8.5	165.8
3	3	17.5	7.5	131.3
4	4	21.0	6.5	68.3
5	4	22.0	8.0	88.0
6	1	24.0	14.5	348.0
7	2	32.0	15.0	240.0
8	1	30.0	11.0	330.0
9	1	20.0	7.0	140.0
10	1	11.0	6.5	71.5
11	4	28.5	9.0	128.3
12	4	31.0	7.0	108.5
13	1	21.0	6.5	136.5
14	6	29.0	4.5	88.7
15	1	24.0	7.5	180.0
16	1	41.0	7.0	287.0

SIMPLE WEDGE TEST - RESULTS OF TEST # 6 - PIECE SIZE

FLOE No.	SHAPE CODE	LENGTH (cm)	WIDTH (cm)	AREA (cm2)
1	1	26.0	4.5	117.0
2	1	9.5	5.0	47.5
3	4	17.0	5.5	46.8
4	7	40.0	9.5	298.5
5	4	28.0	10.0	140.0
6	1	24.0	4.0	96.0
7	1	29.0	10.0	290.0
8	1	30.0	9.5	285.0
9	2	16.0	9.5	76.0
10	2	10.0	7.0	35.0
11	1	13.0	8.0	104.0
12	1	20.0	5.5	110.0
13	1	26.0	4.5	117.0
14	1	18.0	5.0	90.0
15	1	19.0	4.0	76.0
16	2	30.5	13.0	198.3
17	2	14.5	8.0	58.0
18	1	8.0	7.0	56.0
19	2	13.0	8.5	55.3
20	2	9.5	3.0	14.3
21	7	15.0	5.0	58.9
22	1	12.5	3.5	43.8
23	1	33.5	10.0	335.0
24	1	17.0	8.0	136.0

SIMPLE WEDGE TEST - RESULTS OF TEST # 7 - PIECE SIZE

FLOE No.	SHAPE CODE	LENGTH (cm)	WIDTH (cm)	AREA (cm2)
1	1	17.0	11.5	195.5
2	2	17.0	7.5	63.8
3	3	16.5	11.5	189.8
4	1	18.0	10.0	180.0
5	2	24.0	14.0	168.0
6	1	32.0	10.0	320.0
7	7	30.0	10.0	235.6
8	1	16.0	6.0	96.0
9	1	17.5	9.5	166.3
10	4	13.0	6.0	39.0
11	1	21.5	11.0	236.5
12	1	11.0	5.0	55.0
13	7	38.0	9.5	283.5
14	3	16.8	13.0	217.8
15	1	57.0	10.0	570.0
16	7	29.0	8.0	182.2
17	2	15.0	10.5	78.8
18	1	39.0	12.0	468.0
19	5	26.0	9.0	234.0
20	1	19.0	9.5	180.5
21	2	12.0	8.0	48.0
22	3	16.5	13.0	214.5
23	2	26.0	14.0	182.0

SIMPLE WEDGE TEST - RESULTS OF TEST # 8 - PIECE SIZE

FLOE No.	SHAPE CODE	LENGTH (cm)	WIDTH (cm)	AREA (cm2)
1	1	33.0	11.0	363.0
2	3	20.5	10.0	205.0
3	2	20.0	10.0	100.0
4	1	18.0	14.0	252.0
5	2	19.0	12.0	114.0
6	1	6.0	6.0	36.0
7	2	21.0	11.0	115.5
8	4	25.0	12.0	150.0
9	1	24.0	11.0	264.0
10	4	14.0	7.0	49.0
11	1	25.0	11.0	275.0
12	6	38.0	13.0	358.4
13	4	29.0	13.0	188.5
14	7	18.0	7.0	99.0
15	2	28.0	9.0	126.0
16	1	22.0	8.0	176.0
17	7	28.0	12.0	263.9
18	7	17.0	7.0	93.5
19	1	16.0	13.0	208.0
20	7	24.0	12.0	226.2
21	1	20.0	12.0	240.0
22	7	21.0	7.0	115.5
23	2	20.0	8.0	80.0

SIMPLE WEDGE TEST - RESULTS OF TEST # 9 - PIECE SIZE

FLOE No.	SHAPE CODE	LENGTH (cm)	WIDTH (cm)	AREA (cm ²)
1	1	11.0	8.0	88.0
2	4	26.0	10.0	130.0
3	2	50.0	17.0	425.0
4	2	35.0	18.0	315.0
5	2	38.0	10.0	190.0
6	2	30.0	18.0	270.0
7	1	29.0	10.0	290.0
8	1	50.0	18.0	900.0
9	1	56.0	12.0	672.0
10	6	30.0	12.0	268.4
11	2	23.0	8.0	92.0
12	4	24.0	9.0	108.0
13	1	24.0	8.0	192.0
14	2	20.0	5.0	50.0
15	2	8.0	3.0	12.0
16	1	10.0	3.0	30.0
17	1	22.0	6.0	132.0
18	4	11.0	4.0	22.0
19	1	17.0	11.0	187.0
20	1	21.0	13.0	273.0
21	1	19.0	14.0	266.0
22	1	10.0	6.0	60.0
23	1	18.0	3.0	54.0
24	1	52.0	14.0	728.0
25	3	23.0	10.0	230.0
26	4	20.0	9.0	90.0
27	2	9.0	6.0	27.0
28	1	10.0	8.0	80.0

SIMPLE WEDGE TEST - RESULTS OF TEST # 10 - PIECE SIZE

FLOE No.	SHAPE CODE	LENGTH (cm)	WIDTH (cm)	AREA (cm ²)
1	4	26.0	8.0	104.0
2	1	30.0	9.0	270.0
3	2	14.0	8.0	56.0
4	2	14.0	14.0	98.0
5	2	29.0	15.0	217.5
6	3	14.0	12.0	168.0
7	2	6.0	2.0	6.0
8	1	10.0	3.0	30.0
9	1	26.0	5.0	130.0
10	1	21.0	9.0	189.0
11	1	18.0	12.0	216.0
12	3	19.0	21.0	399.0
13	4	22.0	6.0	66.0
14	1	16.0	6.0	96.0
15	4	9.0	3.0	13.5
16	1	15.0	12.0	180.0
17	1	32.0	16.0	512.0

SIMPLE WEDGE TEST - RESULTS OF TEST # 10 - PIECE SIZE, continued

FLOE No.	SHAPE CODE	LENGTH (cm)	WIDTH (cm)	AREA (cm2)
18	1	24.0	19.0	456.0
19	2	14.0	13.0	91.0
20	1	14.0	10.0	140.0
21	1	37.0	6.0	222.0
22	1	24.0	5.0	120.0
23	2	32.0	11.0	176.0
24	4	40.0	11.0	220.0
25	4	25.0	9.0	112.5
26	4	30.0	10.0	150.0
27	4	26.0	7.0	91.0
28	4	45.0	9.0	202.5
29	4	20.0	11.0	110.0
30	1	45.0	10.0	450.0
31	1	37.0	8.0	296.0
32	4	30.0	10.0	150.0
33	2	30.0	11.0	165.0
34	2	10.0	8.0	40.0
35	1	25.0	7.0	175.0
36	1	26.0	12.0	312.0
37	4	20.0	8.0	80.0

SIMPLE WEDGE TEST - RESULTS OF TEST # 11 - PIECE SIZE

FLOE No.	SHAPE CODE	LENGTH (cm)	WIDTH (cm)	AREA (cm2)
1	4	46.0	8.0	184.0
2	5	29.0	4.0	116.0
3	1	36.0	9.0	324.0
4	1	16.0	3.0	48.0
5	1	6.0	5.0	30.0
6	4	31.0	10.0	155.0
7	4	12.0	7.0	42.0
8	1	26.0	6.0	156.0
9	2	13.0	6.0	39.0
10	2	5.0	34.0	85.0
11	1	38.0	6.0	228.0
12	4	27.0	14.0	189.0
13	2	28.0	12.0	168.0
14	1	17.0	3.0	51.0
15	4	20.0	8.0	80.0
16	4	16.0	8.0	64.0
17	1	30.0	7.0	210.0
18	1	24.0	11.0	264.0
19	1	10.0	7.0	70.0
20	1	12.0	10.0	120.0
21	4	19.0	9.0	85.5
22	2	29.0	8.0	116.0
23	1	14.0	4.0	56.0
24	1	37.0	5.0	185.0
25	1	34.0	6.0	204.0

SIMPLE WEDGE TEST - RESULTS OF TEST # 11 - PIECE SIZE, continued

FLOE No.	SHAPE CODE	LENGTH (cm)	WIDTH (cm)	AREA (cm2)
26	1	45.0	5.0	225.0
27	4	33.0	14.0	231.0
28	2	12.0	12.0	72.0
29	6	37.0	8.0	204.5
30	1	46.0	9.0	414.0
31	4	23.0	12.0	138.0
32	2	40.0	21.0	420.0
33	1	3.0	1.0	3.0
34	1	4.0	2.0	8.0
35	1	3.0	1.0	3.0

SIMPLE WEDGE TEST - RESULTS OF TEST # 12 - PIECE SIZE

FLOE No.	SHAPE CODE	LENGTH (cm)	WIDTH (cm)	AREA (cm2)
1	4	31.0	10.0	155.0
2	1	13.0	5.0	65.0
3	1	32.0	9.0	288.0
4	1	15.0	5.0	75.0
5	1	15.0	4.0	60.0
6	1	33.0	7.0	231.0
7	6	29.0	8.0	163.7
8	2	24.0	9.0	108.0
9	1	29.0	10.0	290.0
10	3	11.5	8.0	92.0
11	1	31.0	8.0	248.0
12	1	27.0	10.0	270.0
13	4	11.0	5.0	27.5
14	1	9.0	5.0	45.0
15	1	9.0	4.0	36.0
16	1	15.0	9.0	135.0
17	2	16.0	6.0	48.0
18	4	8.0	5.0	20.0
19	2	8.0	6.0	24.0

SIMPLE WEDGE TEST - RESULTS OF TEST # 13 - PIECE SIZE

FLOE No.	SHAPE CODE	LENGTH (cm)	WIDTH (cm)	AREA (cm2)
1	3	21.0	8.0	168.0
2	4	33.0	11.0	181.5
3	2	30.0	15.0	225.0
4	1	11.0	9.0	99.0
5	2	7.0	24.0	84.0
6	1	34.0	13.0	442.0
7	2	26.0	13.0	169.0
8	1	9.0	4.0	36.0

SIMPLE WEDGE TEST - RESULTS OF TEST # 13 - PIECE SIZE, continued

FLOE No.	SHAPE CODE	LENGTH (cm)	WIDTH (cm)	AREA (cm2)
9	3	14.0	8.0	112.0
10	1	47.0	9.0	423.0
11	2	21.0	12.0	126.0
12	2	22.0	9.0	99.0
13	4	28.0	18.0	252.0
14	4	33.0	15.0	247.5
15	6	25.0	9.0	164.6
16	2	27.0	13.0	175.5
17	4	35.0	14.0	245.0
18	3	46.0	12.0	552.0
19	2	25.0	8.0	100.0
20	1	29.0	10.0	290.0
21	6	24.0	7.0	119.3
22	4	27.0	9.0	121.5
23	2	5.0	2.0	5.0
24	4	25.0	9.0	112.5
25	2	16.0	14.0	112.0
26	6	41.0	12.0	349.5
27	5	22.0	8.0	176.0
28	6	30.0	11.0	242.1
29	4	29.0	8.0	116.0
30	2	28.0	11.0	154.0
31	2	34.0	10.0	170.0

SIMPLE WEDGE TEST - RESULTS OF TEST # 14 - PIECE SIZE

FLOE No.	SHAPE CODE	LENGTH (cm)	WIDTH (cm)	AREA (cm2)
1	2	18.0	9.0	81.0
2	3	35.0	13.0	455.0
3	2	21.0	13.0	136.5
4	2	17.0	10.0	85.0
5	4	21.0	5.0	52.5
6	6	33.0	10.0	235.4
7	2	20.0	8.0	80.0
8	1	25.0	9.0	225.0
9	1	7.0	6.0	42.0
10	1	5.0	2.0	10.0
11	2	37.0	18.0	333.0
12	1	19.0	8.0	152.0
13	7	25.0	7.0	137.4
14	1	5.0	2.0	10.0
15	1	6.0	4.0	24.0
16	1	23.0	9.0	207.0
17	2	20.0	9.0	90.0
18	1	32.0	7.0	224.0
19	6	23.0	5.0	79.5
20	3	13.0	6.0	78.0
21	7	25.0	9.0	176.7

SIMPLE WEDGE TEST - RESULTS OF TEST # 15 - PIECE SIZE

FLOE No.	SHAPE CODE	LENGTH (cm)	WIDTH (cm)	AREA (cm ²)
1	3	33.5	10.0	335.0
2	1	14.0	6.0	84.0
3	2	12.0	23.0	138.0
4	4	9.0	4.0	18.0
5	2	11.0	11.0	60.5
6	2	12.0	7.0	42.0
7	2	27.0	11.0	148.5
8	1	13.0	6.0	78.0
9	2	24.0	12.0	144.0
10	1	32.0	15.0	480.0
11	2	15.0	13.0	97.5
12	2	18.0	11.0	99.0
13	4	30.0	12.0	180.0
14	1	25.0	9.0	225.0
15	4	18.0	10.0	90.0
16	2	10.0	6.0	30.0
17	2	34.0	11.0	187.0
18	7	15.0	9.0	106.0
19	7	21.0	10.0	164.9
20	1	7.0	3.0	21.0
21	1	13.0	10.0	130.0
22	4	15.0	12.0	90.0
23	6	36.0	15.0	405.9
24	2	14.0	34.0	238.0
25	2	27.0	11.0	148.5
26	2	13.0	11.0	71.5
27	4	26.0	15.0	195.0
28	1	8.0	6.0	48.0
29	3	19.5	17.0	331.5

SIMPLE WEDGE TEST - RESULTS OF TEST # 16 - PIECE SIZE

FLOE No.	SHAPE CODE	LENGTH (cm)	WIDTH (cm)	AREA (cm ²)
1	2	31.0	11.0	170.5
2	2	21.0	14.0	147.0
3	7	14.0	4.0	44.0
4	4	17.0	9.0	76.5
5	2	12.0	9.0	54.0
6	3	32.0	12.0	384.0
7	1	5.0	3.0	15.0
8	5	13.0	4.0	52.0
9	1	15.0	13.0	195.0
10	2	15.0	10.0	75.0
11	7	14.0	5.0	55.0

SIMPLE WEDGE TEST - RESULTS OF TEST # 16 - PIECE SIZE, continued

FLOE No.	SHAPE CODE	LENGTH (cm)	WIDTH (cm)	AREA (cm2)
12	6	20.0	7.0	101.9
13	3	9.5	8.0	76.0
14	4	16.0	6.0	48.0
15	2	14.0	10.0	70.0
16	5	12.0	6.0	72.0
17	2	10.0	8.0	40.0
18	1	3.0	3.0	9.0
19	1	4.0	3.0	12.0
20	1	4.0	2.0	8.0
21	1	4.0	2.0	8.0
22	1	5.0	2.0	10.0
23	2	4.0	4.0	8.0
24	1	1.0	1.0	1.0
25	4	15.0	6.0	45.0
26	4	22.0	13.0	143.0
27	2	7.0	20.0	70.0
28	7	35.0	14.0	384.8
29	2	10.0	7.0	35.0
30	6	22.0	9.0	148.3
31	5	9.0	4.0	36.0
32	7	8.0	4.0	25.1
33	2	15.0	10.0	75.0
34	4	11.0	5.0	27.5
35	4	10.0	4.0	20.0
36	1	11.0	6.0	66.0
37	4	4.0	2.0	4.0
38	1	8.0	8.0	64.0
39	1	22.0	6.0	132.0
40	3	3.5	3.0	10.5
41	2	6.0	6.0	18.0
42	1	14.0	7.0	98.0
43	4	13.0	6.0	39.0
44	2	5.0	2.0	5.0
45	1	2.0	2.0	4.0
46	5	14.0	5.0	70.0
47	1	2.0	2.0	4.0
48	3	14.0	14.0	196.0
49	7	21.0	9.0	148.4
50	1	16.0	10.0	160.0
51	4	11.0	7.0	38.5
52	2	9.0	6.0	27.0
53	4	11.0	4.0	22.0
54	2	10.0	6.0	30.0
55	1	3.0	2.0	6.0
56	1	5.0	3.0	15.0
57	2	11.0	8.0	44.0
58	6	19.0	7.0	97.7
59	4	10.0	6.0	30.0
60	2	7.0	6.0	21.0

SIMPLE WEDGE TEST - RESULTS OF TEST # 17 - PIECE SIZE

FLOE No.	SHAPE CODE	LENGTH (cm)	WIDTH (cm)	AREA (cm ²)
1	7	30.0	8.0	188.5
2	7	24.0	6.0	113.1
3	2	11.0	27.0	148.5
4	7	28.0	9.0	197.9
5	3	18.0	12.0	216.0
6	2	11.0	10.0	55.0
7	2	14.0	11.0	77.0
8	2	13.0	13.0	84.5
9	6	21.0	7.0	106.2
10	2	27.0	10.0	135.0
11	1	15.0	12.0	180.0
12	2	21.0	7.0	73.5
13	3	9.5	20.0	190.0
14	1	25.0	16.0	400.0
15	4	25.0	17.0	212.5
16	2	18.0	14.0	126.0
17	2	16.0	6.0	48.0
18	1	10.0	5.0	50.0
19	2	12.0	11.0	66.0
20	2	8.0	8.0	32.0
21	2	11.0	8.0	44.0
22	3	20.0	11.0	220.0
23	7	21.0	11.0	181.4
24	4	29.0	10.0	145.0
25	2	16.0	12.0	96.0
26	3	15.0	8.0	120.0
27	2	30.0	10.0	150.0
28	2	24.0	9.0	108.0
29	1	15.0	6.0	90.0
30	6	23.0	6.0	96.8
31	1	10.0	5.0	50.0
32	2	21.0	7.0	73.5
33	2	14.0	11.0	77.0
34	2	21.0	13.0	136.5
35	4	16.0	4.0	32.0

SIMPLE WEDGE TEST - RESULTS OF TEST # 18 - PIECE SIZE

FLOE No.	SHAPE CODE	LENGTH (cm)	WIDTH (cm)	AREA (cm ²)
1	2	30.0	14.0	210.0
2	2	12.0	11.0	66.0
3	7	24.0	8.0	150.8
4	4	14.0	7.0	49.0
5	7	26.0	10.0	204.2
6	5	20.0	7.0	140.0
7	3	15.0	8.0	120.0
8	4	17.0	10.0	85.0
9	2	11.0	7.0	38.5
10	1	15.0	6.0	90.0

SIMPLE WEDGE TEST - RESULTS OF TEST # 18 - PIECE SIZE, continued

FLOE No.	SHAPE CODE	LENGTH (cm)	WIDTH (cm)	AREA (cm ²)
11	7	15.0	8.0	94.2
12	4	18.0	6.0	54.0
13	3	12.0	9.0	108.0
14	1	12.0	11.0	132.0
15	1	13.0	8.0	104.0
16	4	23.0	9.0	103.5
17	4	11.0	7.0	38.5
18	1	16.0	8.0	128.0
19	7	18.0	4.0	56.5
20	2	18.0	15.0	135.0
21	7	15.0	3.0	35.3
22	3	20.5	13.0	266.5
23	3	10.0	9.0	90.0
24	4	16.0	10.0	80.0
25	3	8.0	14.0	112.0
26	2	11.0	11.0	60.5
27	3	25.5	16.0	408.0
28	2	13.0	9.0	58.5
29	1	17.0	12.0	204.0
30	4	25.0	16.0	200.0
31	6	32.0	9.0	203.7
32	2	21.0	6.0	63.0
33	3	8.5	11.0	93.5
34	4	22.0	12.0	132.0

SIMPLE WEDGE TEST - RESULTS OF TEST # 19 - PIECE SIZE

FLOE No.	SHAPE CODE	LENGTH (cm)	WIDTH (cm)	AREA (cm ²)
1	7	51.0	15.0	600.8
2	6	56.0	19.0	770.9
3	7	34.0	20.0	534.1
4	2	25.0	12.0	150.0
5	5	27.0	6.0	162.0
6	7	20.0	10.0	157.1
7	1	20.0	11.0	220.0
8	2	46.0	17.0	391.0
9	2	25.0	15.0	187.5
10	3	17.0	17.0	289.0
11	2	27.0	13.0	175.5
12	1	16.0	7.0	112.0
13	2	34.0	12.0	204.0
14	4	16.0	12.0	96.0
15	2	22.0	10.0	110.0
16	2	34.0	14.0	238.0
17	2	53.0	20.0	530.0
18	4	20.0	11.0	110.0
19	7	58.0	12.0	546.6
20	6	24.0	10.0	180.4
21	4	18.0	10.0	90.0

SIMPLE WEDGE TEST - RESULTS OF TEST # 20 - PIECE SIZE

FLOE No.	SHAPE CODE	LENGTH (cm)	WIDTH (cm)	AREA (cm2)
1	4	45.0	17.0	382.5
2	5	37.0	11.0	407.0
3	5	48.0	12.0	576.0
4	1	34.0	16.0	544.0
5	1	29.0	11.0	319.0
6	2	42.0	17.0	357.0
7	1	28.0	16.0	448.0
8	7	13.0	8.0	81.7
9	7	60.0	12.0	565.5
10	7	44.0	12.0	414.7
11	7	32.0	8.0	201.1
12	4	34.0	14.0	238.0
13	1	40.0	17.0	680.0
14	7	16.0	7.0	88.0
15	7	25.0	10.0	196.3
16	7	21.0	10.0	164.9

SIMPLE WEDGE TEST - RESULTS OF TEST # 22 - PIECE SIZE

FLOE No.	SHAPE CODE	LENGTH (cm)	WIDTH (cm)	AREA (cm2)
1	2	72.0	20.0	720.0
2	4	19.0	10.0	95.0
3	1	49.0	12.0	588.0
4	4	20.0	12.0	120.0
5	7	19.0	8.0	119.4
6	6	26.0	10.0	192.4
7	1	12.0	7.0	84.0
8	2	29.0	13.0	188.5
9	2	48.0	20.0	480.0
10	7	50.0	11.0	432.0
11	2	28.0	23.0	322.0
12	2	41.0	22.0	451.0
13	1	53.0	16.0	848.0
14	1	20.0	9.0	180.0
15	1	10.0	6.0	60.0
16	7	77.0	25.0	1511.9

SIMPLE WEDGE TEST - RESULTS OF TEST # 23 - PIECE SIZE

FLOE No.	SHAPE CODE	LENGTH (cm)	WIDTH (cm)	AREA (cm2)
1	1	27.0	18.0	486.0
2	7	36.0	12.0	339.3
3	7	30.0	10.0	235.6
4	2	35.0	17.0	297.5
5	1	36.0	14.0	504.0
6	2	36.0	17.0	306.0
7	4	20.0	13.0	130.0
8	1	20.0	12.0	240.0
9	2	51.0	14.0	357.0
10	7	64.0	23.0	1156.1
11	1	18.0	8.0	144.0
12	1	16.0	13.0	208.0
13	1	28.0	9.0	252.0
14	2	24.0	14.0	168.0
15	2	23.0	13.0	149.5
16	4	15.0	6.0	45.0
17	2	11.0	5.0	27.5
18	2	17.0	7.0	59.5
19	1	6.0	6.0	36.0

SIMPLE WEDGE TEST - RESULTS OF TEST # 24 - PIECE SIZE

FLOE No.	SHAPE CODE	LENGTH (cm)	WIDTH (cm)	AREA (cm2)
1	1	42.0	14.0	588.0
2	1	33.0	7.0	231.0
3	6	46.0	18.0	614.7
4	4	18.0	12.0	108.0
5	7	27.0	8.0	169.6
6	7	34.0	12.0	320.4
7	1	44.0	10.0	440.0
8	1	32.0	10.0	320.0
9	7	30.0	11.0	259.2
10	2	24.0	12.0	144.0
11	1	36.0	11.0	396.0
12	7	40.0	12.0	377.0
13	2	22.0	16.0	176.0
14	2	26.0	12.0	156.0
15	2	21.0	22.0	231.0
16	2	15.0	6.0	45.0
17	2	30.0	11.0	165.0
18	2	26.0	11.0	143.0

SIMPLE WEDGE TEST - RESULTS OF TEST # 25 - PIECE SIZE

FLOE No.	SHAPE CODE	LENGTH (cm)	WIDTH (cm)	AREA (cm ²)
1	7	54.0	7.0	296.9
2	7	32.0	13.0	326.7
3	2	32.0	12.0	192.0
4	1	30.0	10.0	300.0
5	2	19.0	10.0	95.0
6	2	34.0	11.0	187.0
7	7	31.0	17.0	413.9
8	7	18.0	14.0	197.9
9	6	21.0	9.0	142.9
10	1	12.0	9.0	108.0
11	1	16.0	11.0	176.0
12	1	31.0	14.0	434.0
13	1	44.0	12.0	528.0
14	2	35.0	14.0	245.0
15	4	19.0	10.0	95.0
16	2	14.0	14.0	98.0
17	7	24.0	10.0	188.5
18	5	15.0	8.0	120.0
19	1	28.0	9.0	252.0
20	6	32.0	8.0	178.9
21	1	14.0	10.0	140.0
22	3	7.0	9.0	63.0
23	1	17.0	3.0	51.0

SIMPLE WEDGE TEST - RESULTS OF TEST # 26 - PIECE SIZE

FLOE No.	SHAPE CODE	LENGTH (cm)	WIDTH (cm)	AREA (cm ²)
1	4	30.0	12.0	180.0
2	4	27.0	12.0	162.0
3	7	17.0	9.0	120.2
4	7	18.0	10.0	141.4
5	4	21.0	11.0	115.5
6	7	18.0	10.0	141.4
7	4	30.0	9.0	135.0
8	7	38.0	14.0	417.8
9	4	16.0	11.0	88.0
10	2	26.0	13.0	169.0
11	4	28.0	13.0	182.0
12	4	23.0	12.0	138.0
13	1	15.0	12.0	180.0
14	4	28.0	10.0	140.0
15	1	18.0	8.0	144.0
16	1	21.0	10.0	210.0
17	1	32.0	7.0	224.0
18	7	16.0	7.0	88.0
19	2	14.0	9.0	63.0
20	2	10.0	10.0	50.0

SIMPLE WEDGE TEST - RESULTS OF TEST # 27 - PIECE SIZE

FLOE No.	SHAPE CODE	LENGTH (cm)	WIDTH (cm)	AREA (cm2)
1	7	39.0	13.0	398.2
2	1	25.0	7.0	175.0
3	7	25.0	6.0	117.8
4	2	20.0	11.0	110.0
5	7	47.0	14.0	516.8
6	7	31.0	10.0	243.5
7	1	39.0	9.0	351.0
8	6	45.0	10.0	311.5
9	2	32.0	11.0	176.0
10	6	30.0	7.0	145.9
11	1	39.0	13.0	507.0
12	5	48.0	7.0	336.0
13	6	21.0	8.0	124.1
14	6	49.0	10.0	337.3
15	7	23.0	7.0	126.4
16	2	21.0	8.0	84.0
17	5	58.0	11.0	638.0
18	7	44.0	10.0	345.6
19	1	28.0	10.0	280.0
20	5	18.0	6.0	108.0
21	2	16.0	6.0	48.0
22	1	12.0	12.0	144.0

SIMPLE WEDGE TEST - RESULTS OF TEST # 28 - PIECE SIZE

FLOE No.	SHAPE CODE	LENGTH (cm)	WIDTH (cm)	AREA (cm2)
1	7	45.0	12.0	424.1
2	7	18.0	9.0	127.2
3	7	38.0	11.0	328.3
4	4	17.0	10.0	85.0
5	7	26.0	6.0	122.5
6	5	53.0	10.0	530.0
7	2	29.0	9.0	130.5
8	7	38.0	9.0	268.6
9	2	13.0	6.0	39.0
10	6	14.0	3.0	29.0
11	6	34.0	13.0	326.7
12	7	25.0	10.0	196.3
13	6	18.0	8.0	109.8
14	6	26.0	9.0	170.1
15	2	36.0	15.0	270.0
16	4	35.0	12.0	210.0
17	7	25.0	8.0	157.1

SIMPLE WEDGE TEST - RESULTS OF TEST # 29 - PIECE SIZE

FLOE No.	SHAPE CODE	LENGTH (cm)	WIDTH (cm)	AREA (cm ²)
1	7	41.0	11.0	354.2
2	2	24.0	9.0	108.0
3	7	28.0	10.0	219.9
4	6	36.0	10.0	254.2
5	6	45.0	9.0	278.5
6	2	10.0	24.0	120.0
7	2	29.0	9.0	130.5
8	2	30.0	6.0	90.0
9	1	37.0	9.0	333.0
10	1	31.0	7.0	217.0
11	7	31.0	7.0	170.4
12	7	23.0	4.0	72.3
13	4	17.0	8.0	68.0
14	4	28.0	13.0	182.0
15	7	21.0	7.0	115.5
16	7	35.0	7.0	192.4

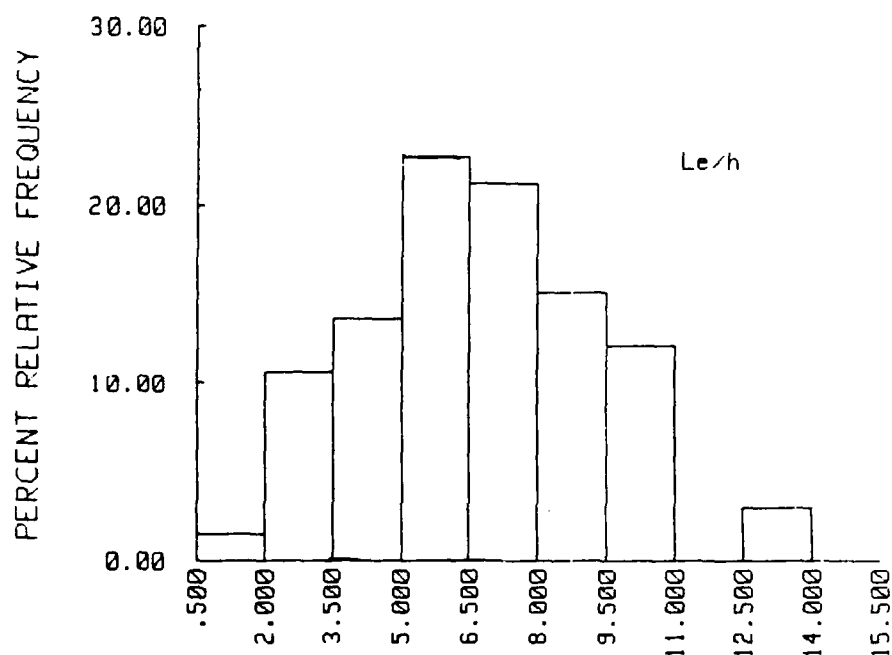
SIMPLE WEDGE TEST - RESULTS OF TEST # 30 - PIECE SIZE

FLOE No.	SHAPE CODE	LENGTH (cm)	WIDTH (cm)	AREA (cm ²)
1	1	34.0	10.0	340.0
2	7	31.0	10.0	243.5
3	2	23.0	10.0	115.0
4	6	35.0	10.0	247.9
5	7	36.0	8.0	226.2
6	7	28.0	7.0	153.9
7	7	23.0	6.0	108.4
8	5	28.0	9.0	252.0
9	5	16.0	11.0	176.0
10	1	34.0	9.0	306.0
11	7	47.0	14.0	516.8
12	2	28.0	12.0	168.0
13	7	38.0	10.0	298.5
14	1	19.0	7.0	133.0
15	2	45.0	16.0	360.0
16	2	23.0	8.0	92.0
17	2	24.0	12.0	144.0
18	1	23.0	8.0	184.0
19	7	30.0	15.0	353.4

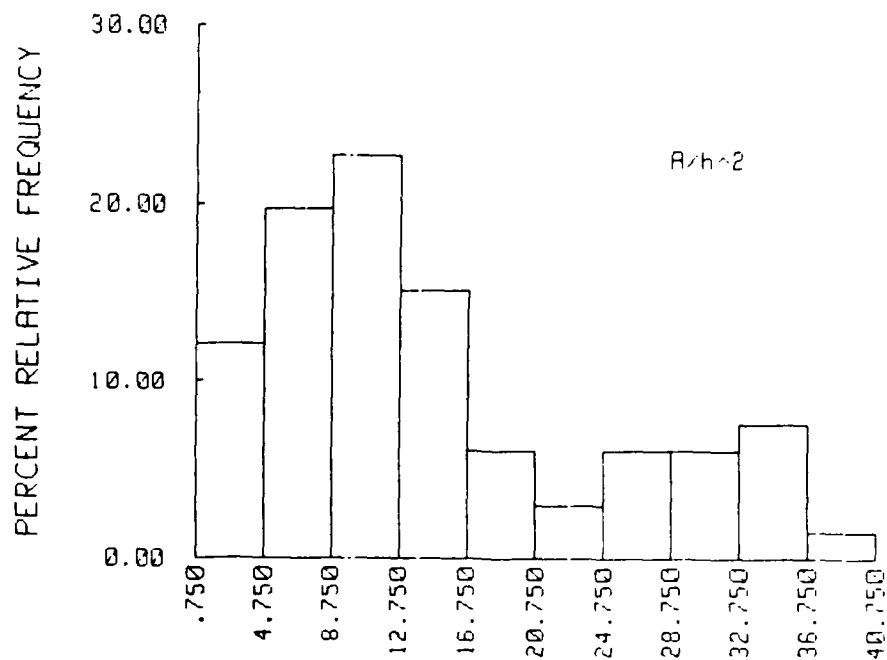
APPENDIX B: WEDGE TESTS—HISTOGRAMS OF FLOE LENGTH AND FLOE AREA

TESTS IN ICE SHEET No. 2 - TESTS 4 to 6

HISTOGRAM

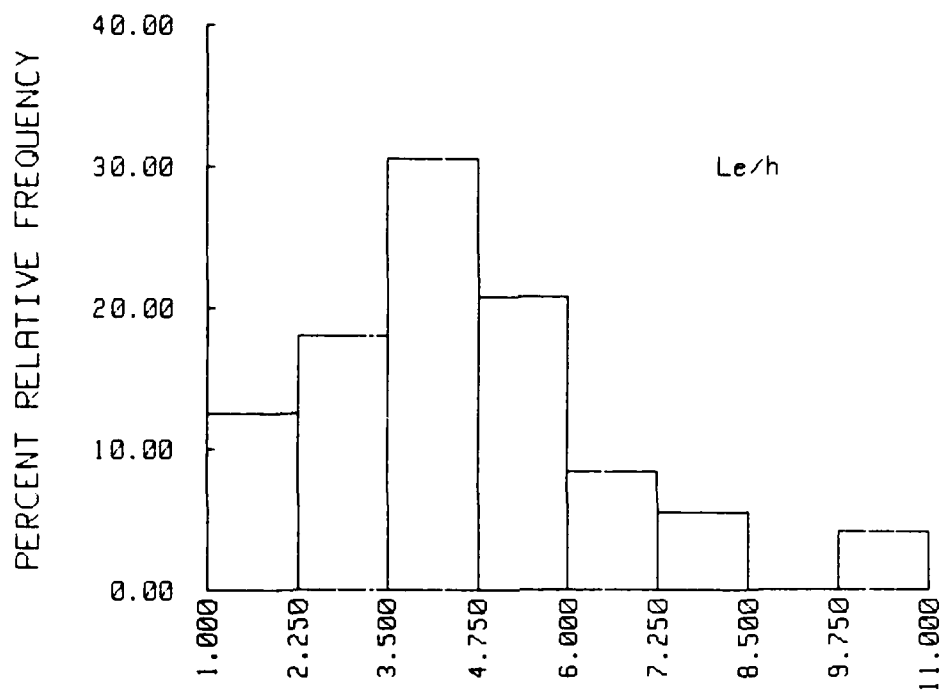


HISTOGRAM

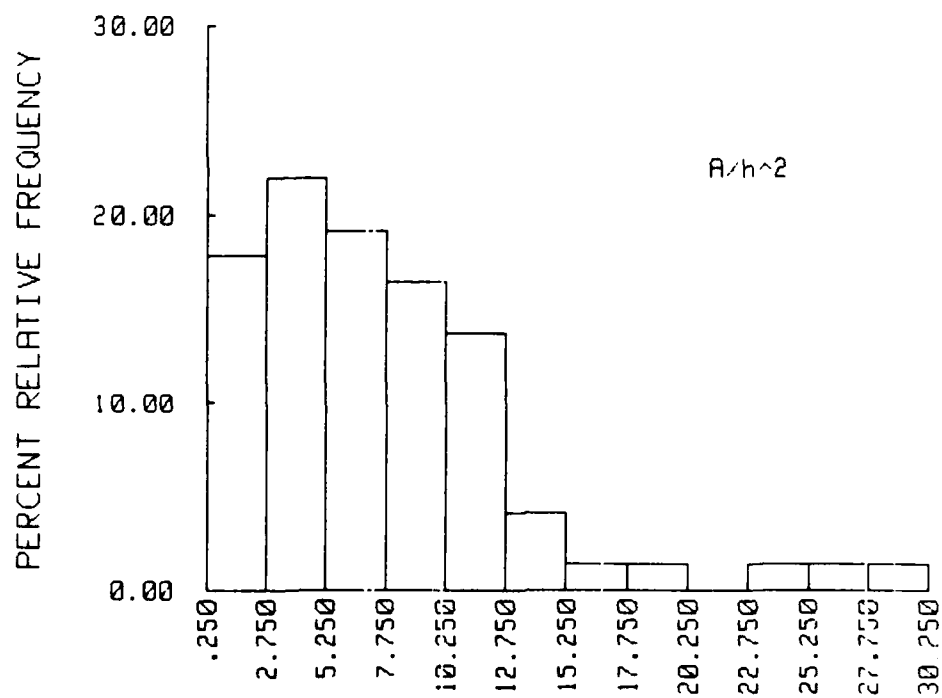


TESTS IN ICE SHEET No. 3 - TESTS 7 to 9

HISTOGRAM

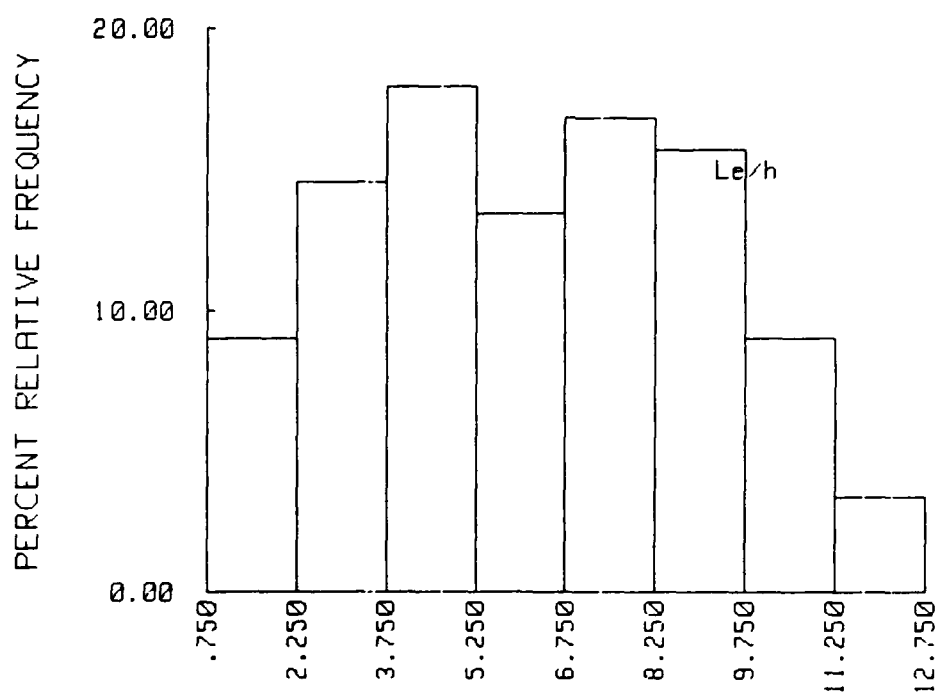


HISTOGRAM

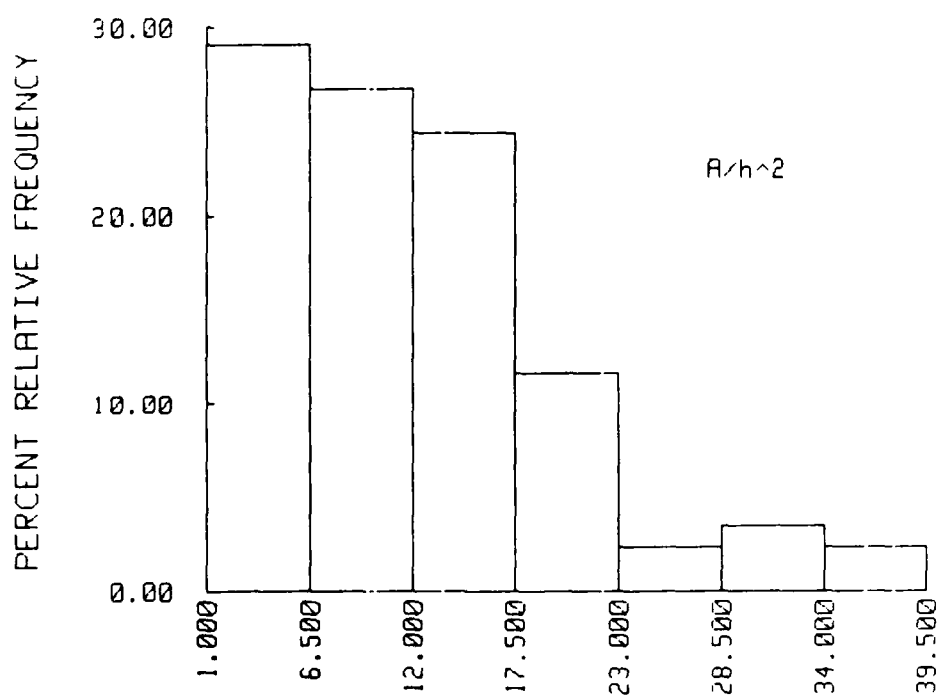


TESTS IN ICE SHEET No. 4 - TESTS 10 to 12

HISTOGRAM

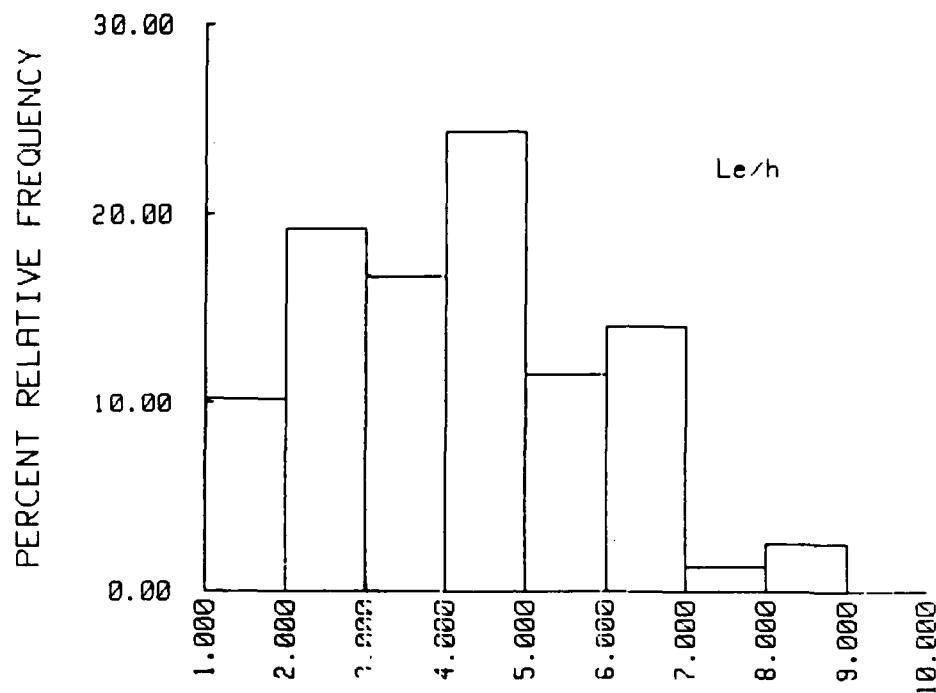


HISTOGRAM

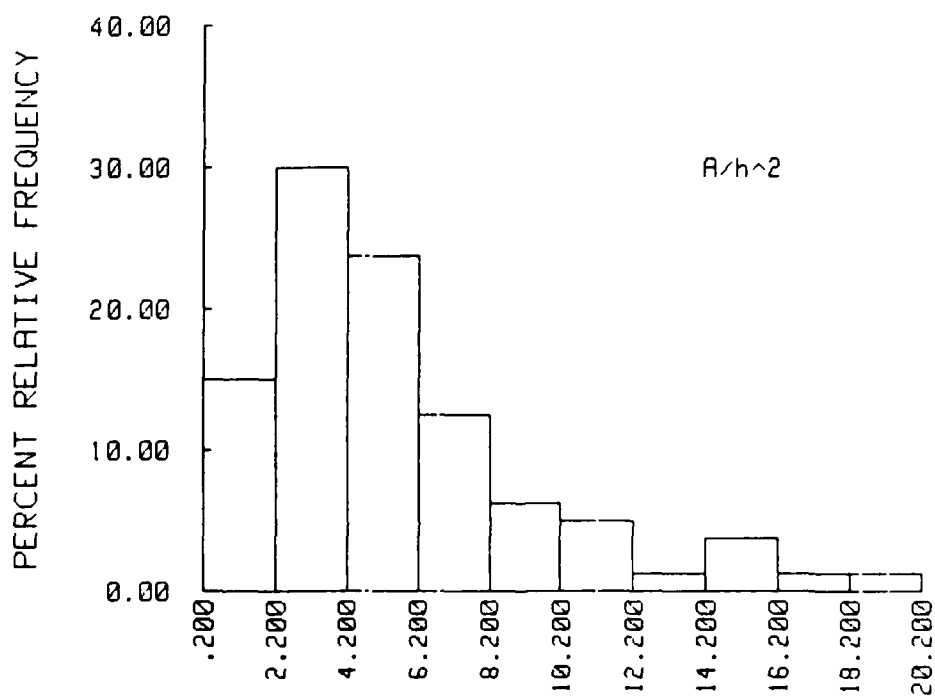


TESTS IN ICE SHEET No. 5 - TESTS 13 to 15

HISTOGRAM

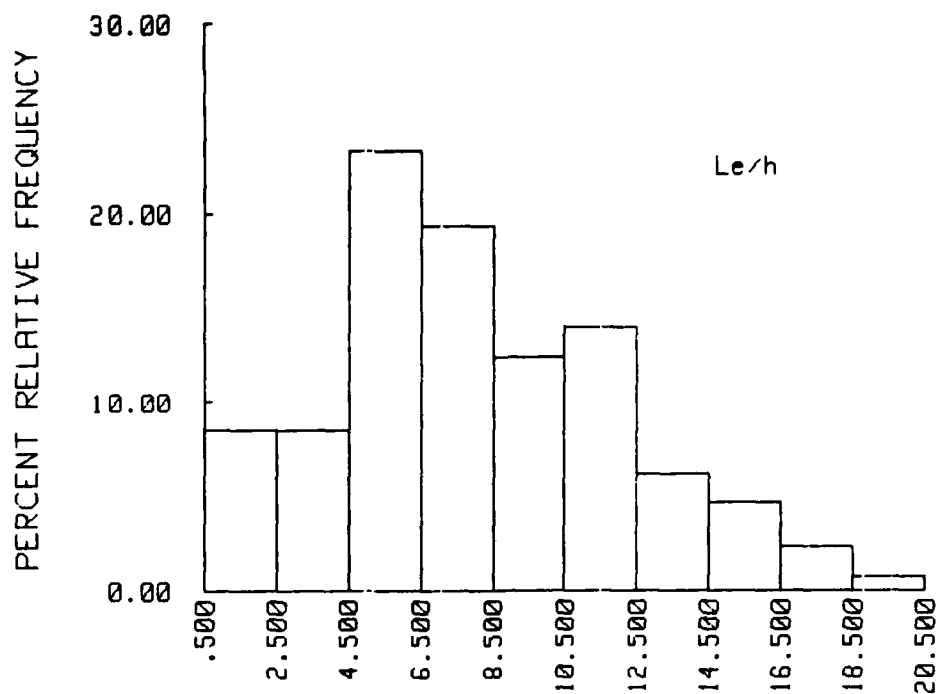


HISTOGRAM



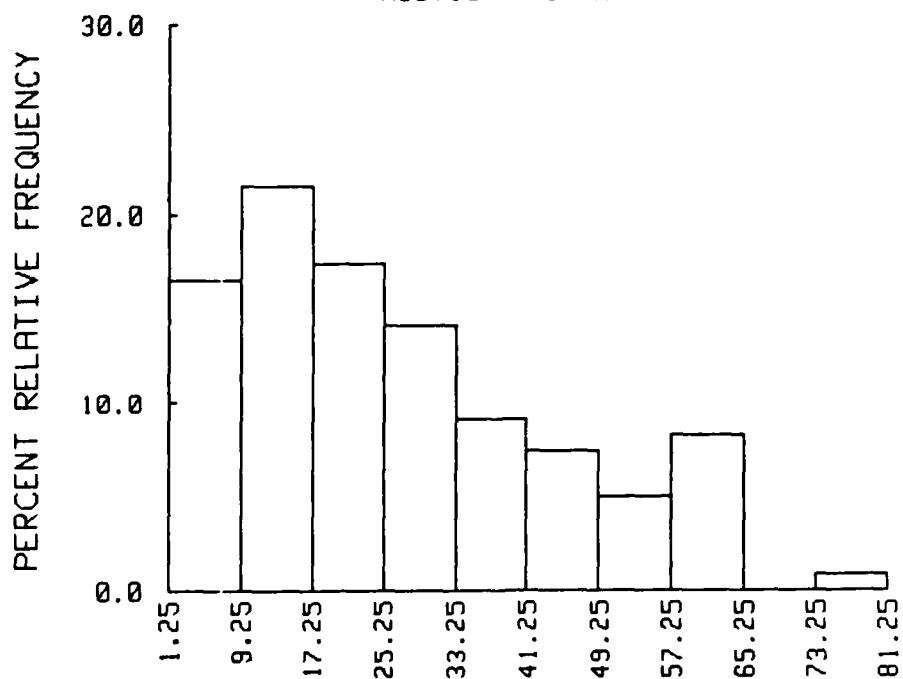
TESTS IN ICE SHEET No. 6 - TESTS 16 to 18

HISTOGRAM



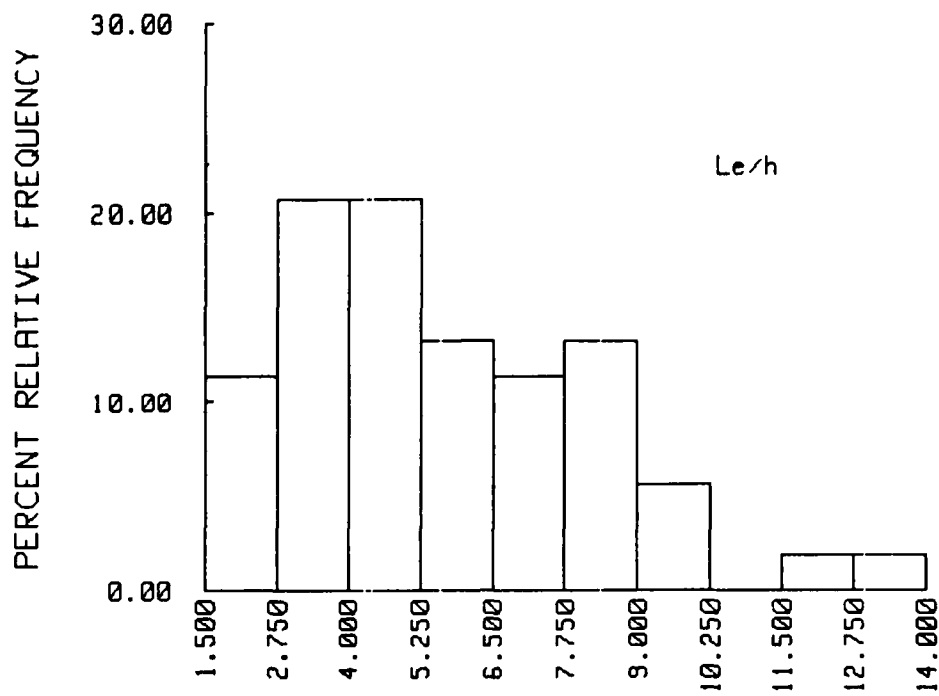
SIMPLE WEDGE TESTS - TESTS 16 TO 18

HISTOGRAM on A/h^2

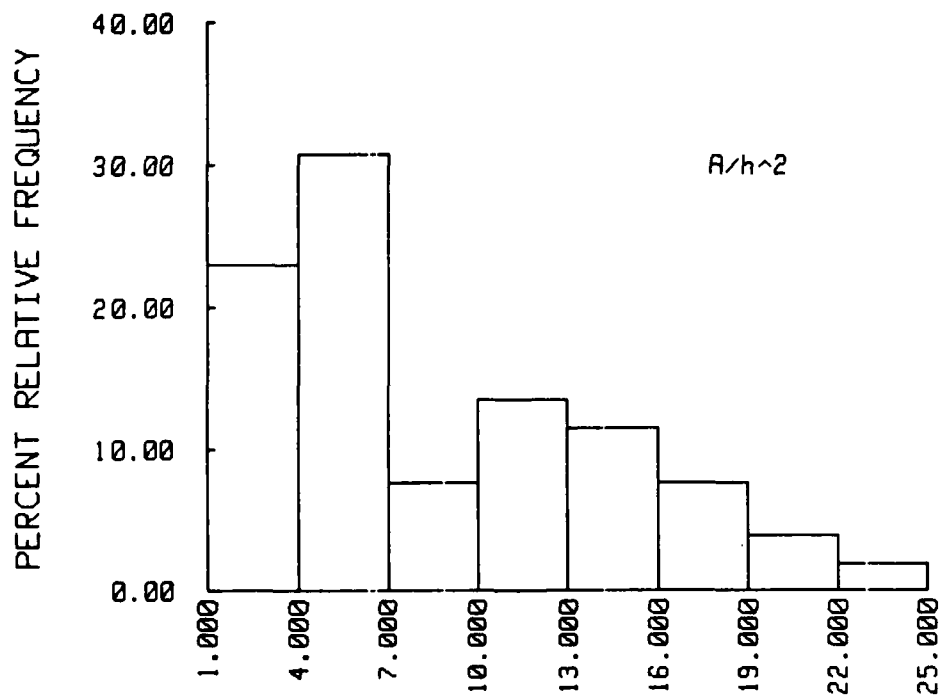


TESTS IN ICE SHEET No. 7 - TESTS 19 to 22

HISTOGRAM

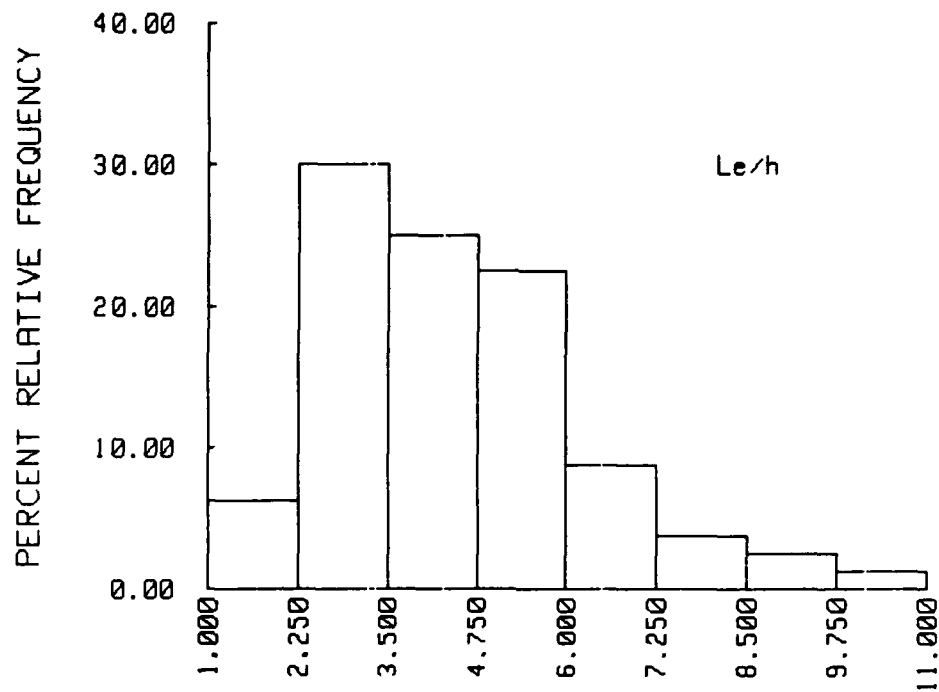


HISTOGRAM

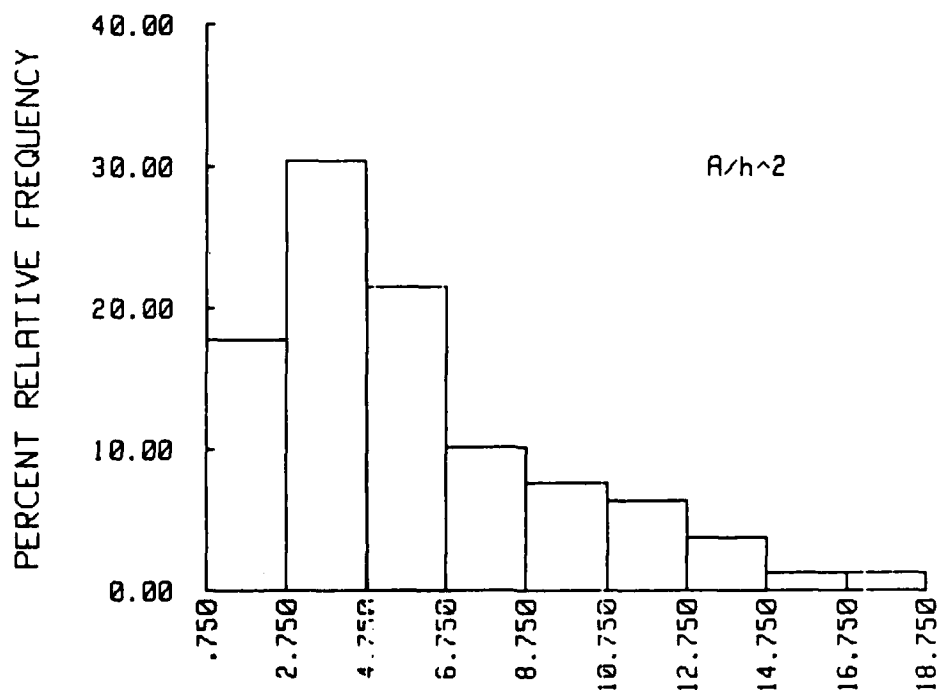


TESTS IN ICE SHEET No. 8 - TESTS 23 to 26

HISTOGRAM

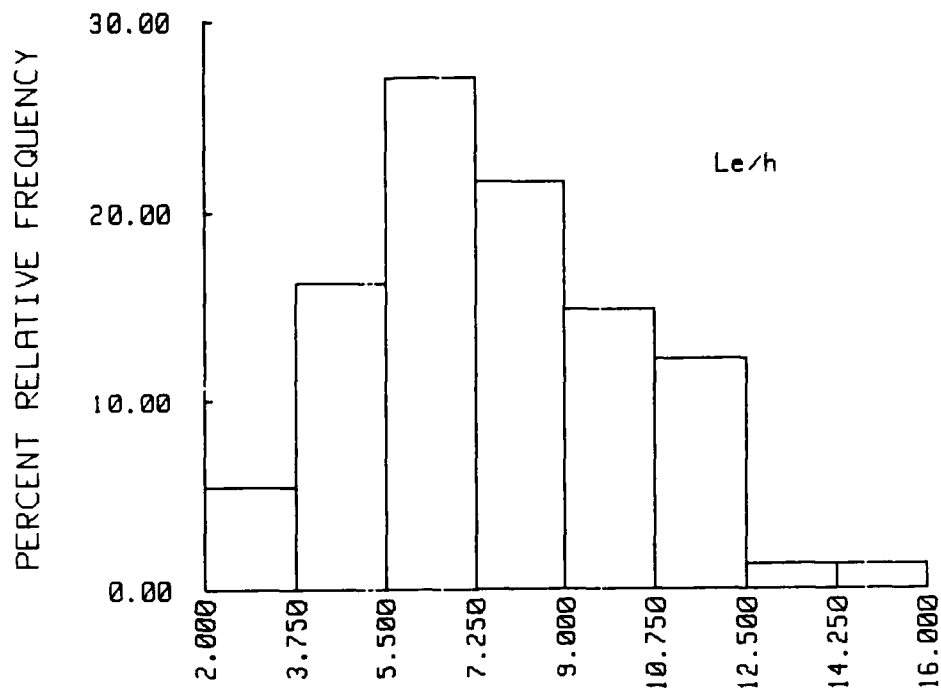


HISTOGRAM

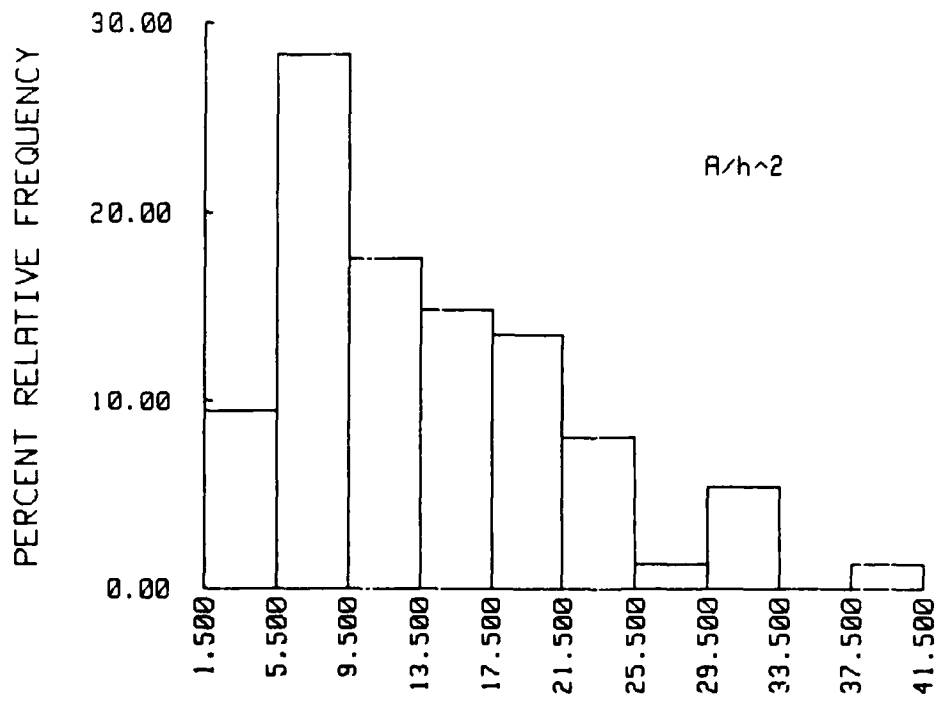


TESTS IN ICE SHEET No. 9 - TESTS 27 to 30

HISTOGRAM

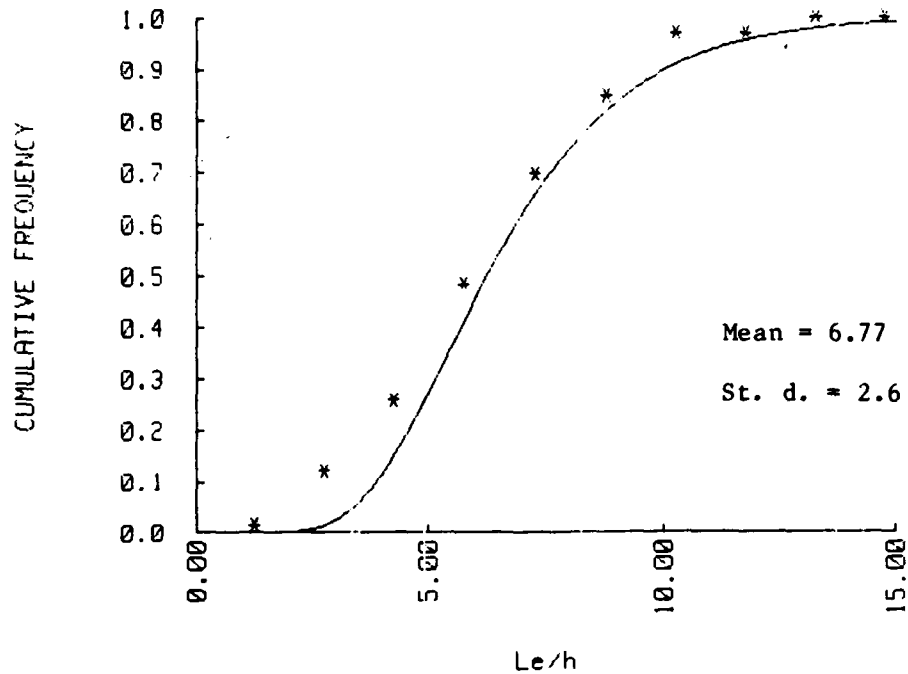


HISTOGRAM

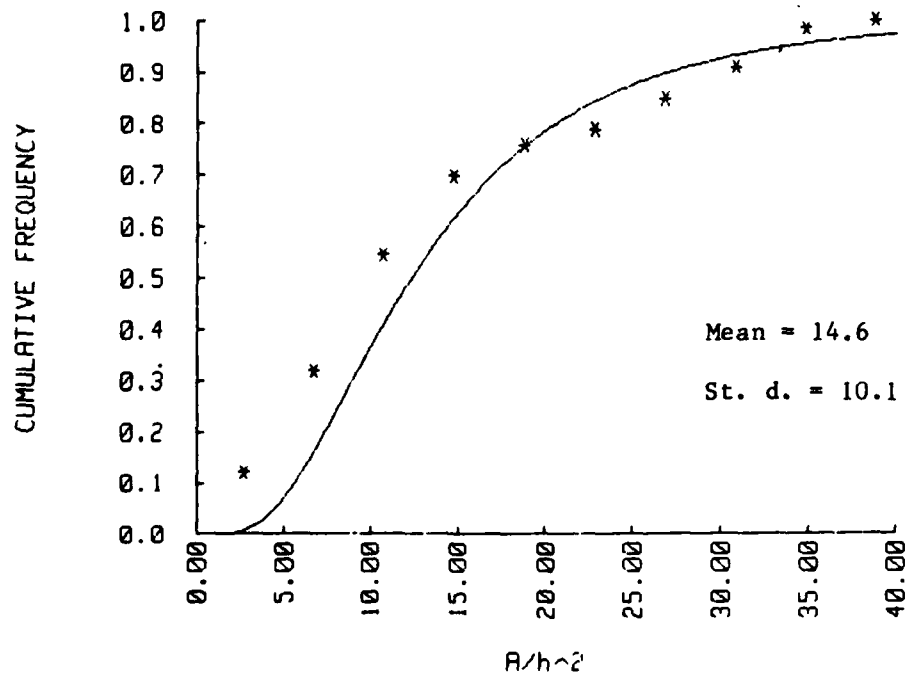


**APPENDIX C: CUMULATIVE FREQUENCY DISTRIBUTIONS
FOR FLOE LENGTH L/H AND FLOE AREA A/H^2
(Current Study)**

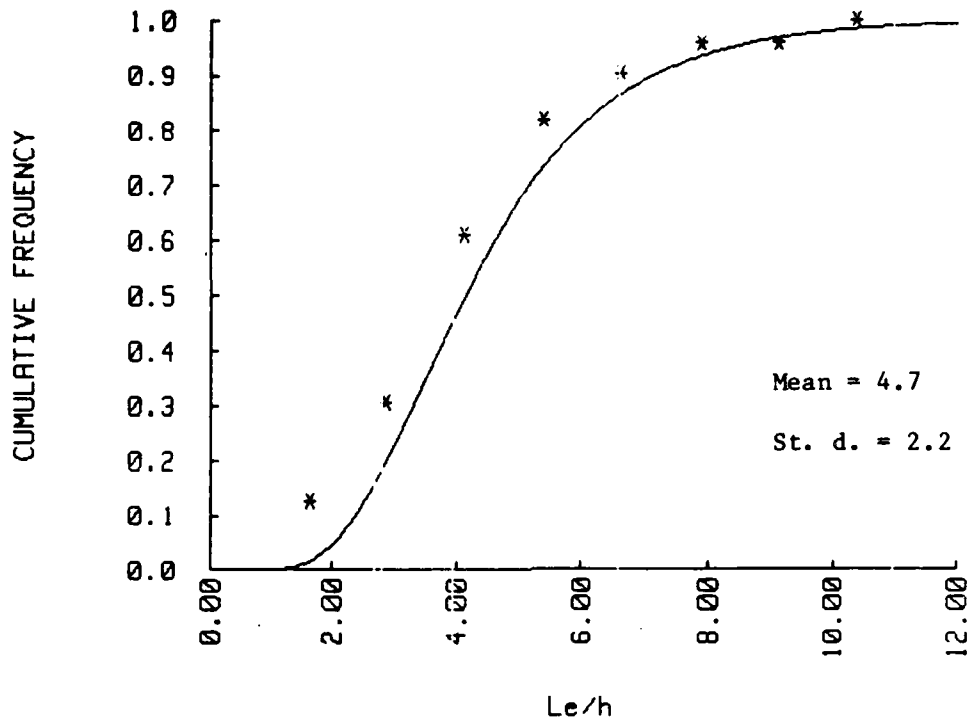
WEDGE TESTS # 4 TO 6: L_e/h



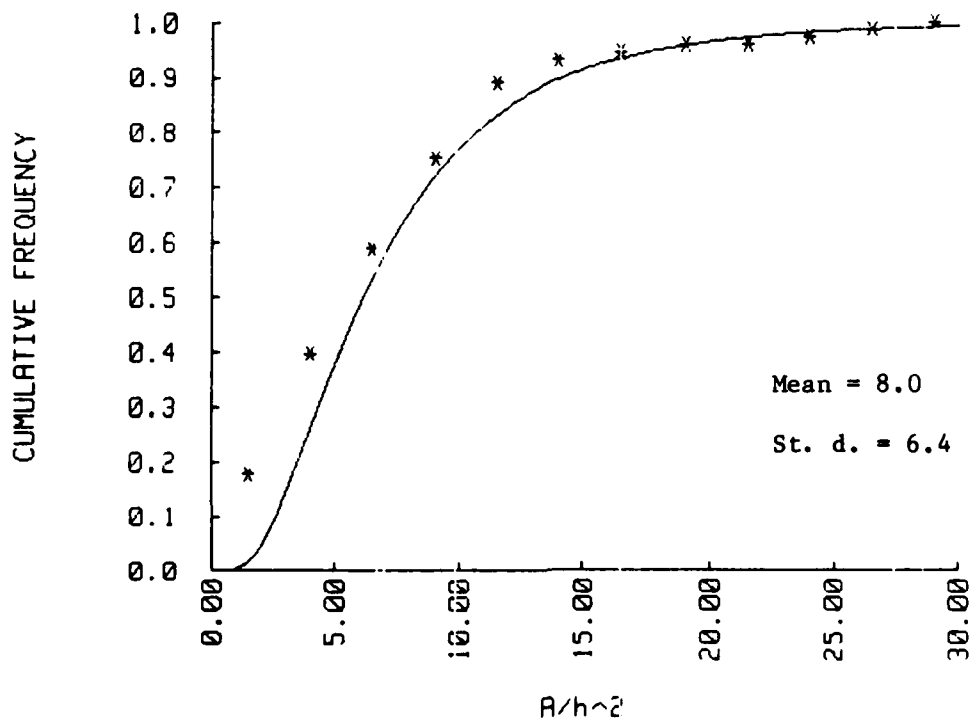
WEDGE TESTS # 4 TO 6: A/h^2



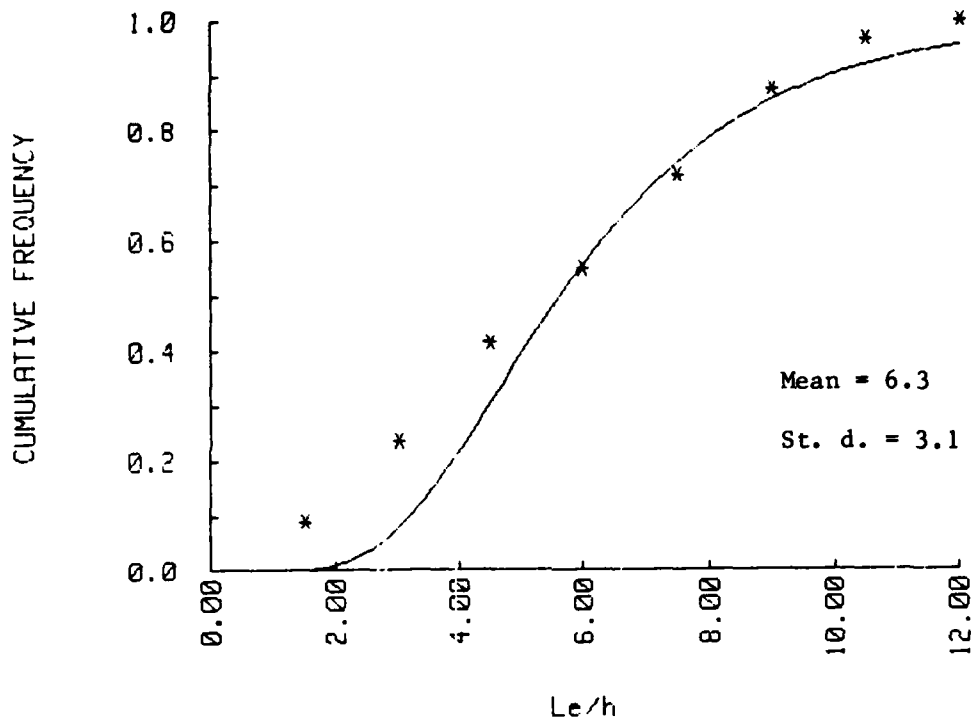
WEDGE TESTS # 7 TO 9: L_e/h



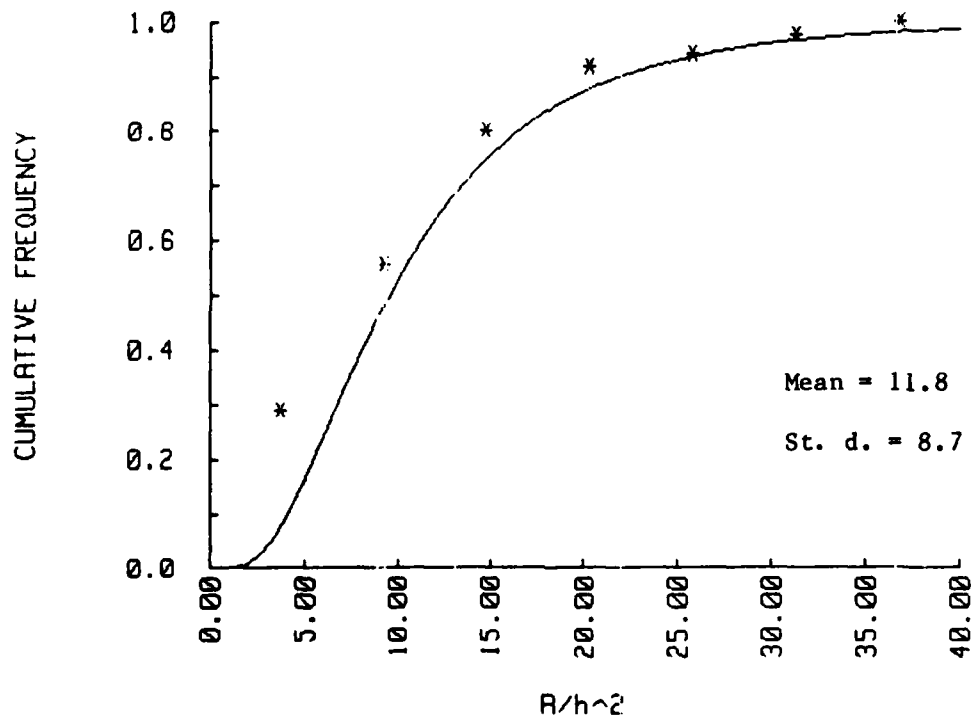
WEDGE TESTS # 7 TO 9: A/h^2



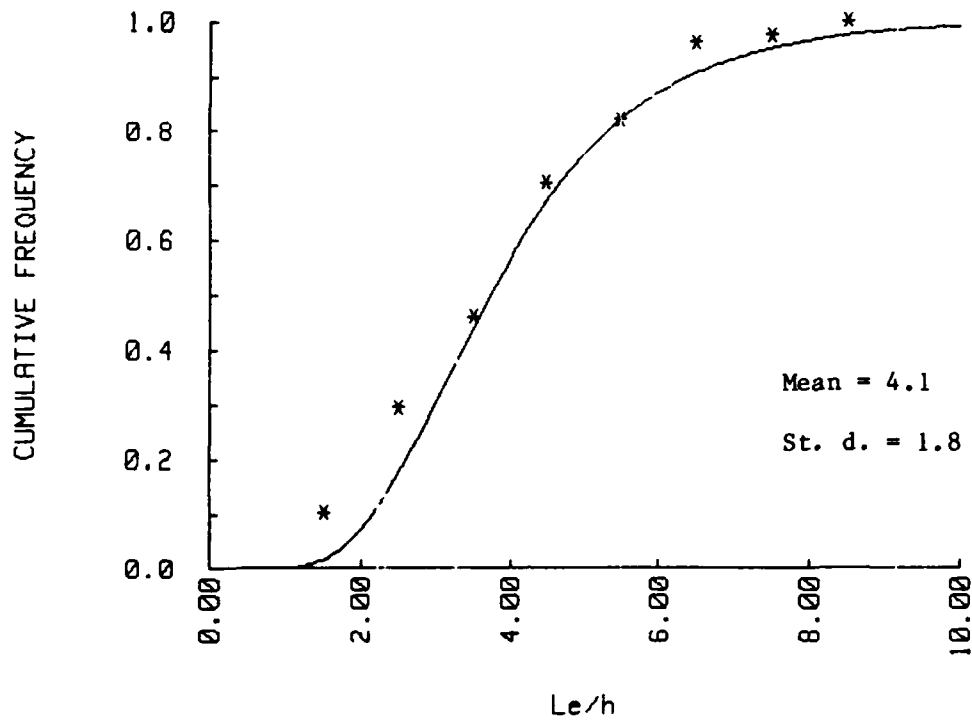
WEDGE TESTS # 10-12: L_e/h



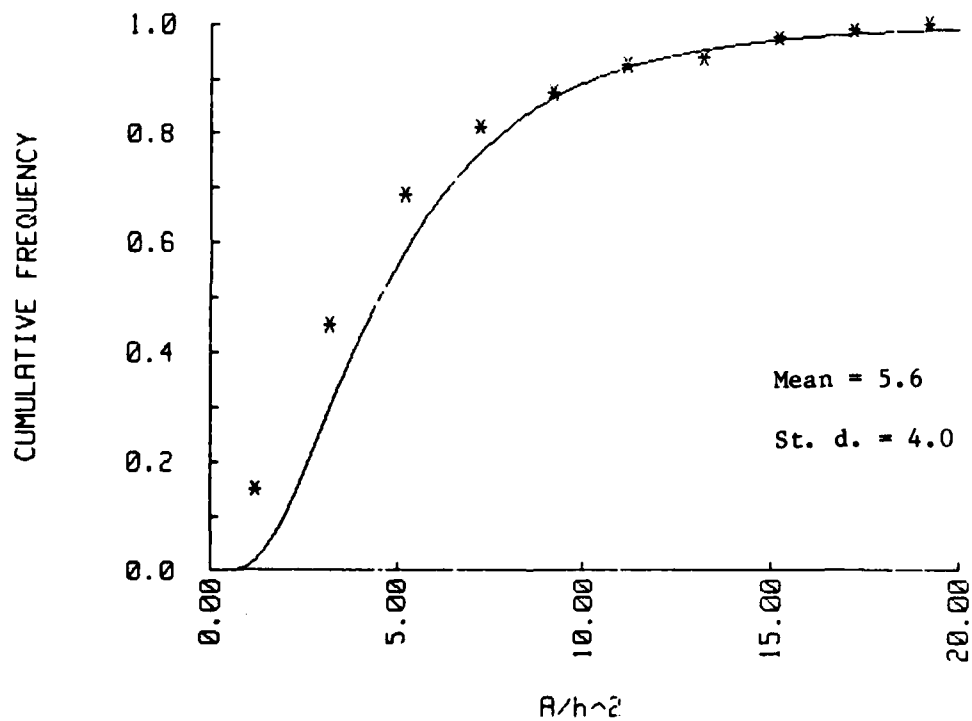
WEDGE TESTS # 10 TO 12: R/h^2



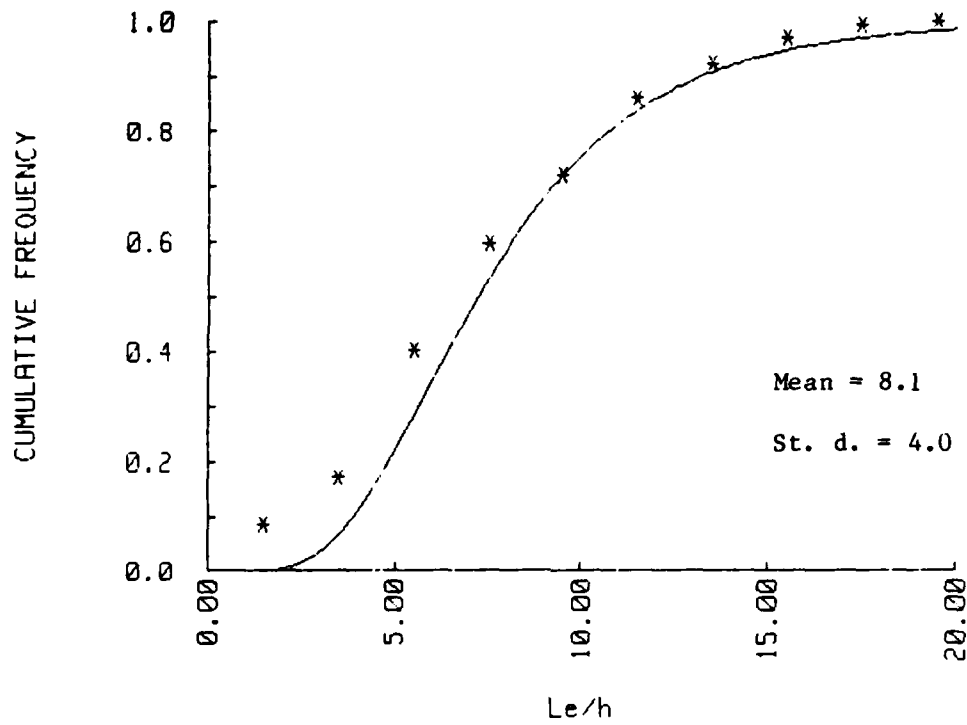
WEDGE TESTS # 13 TO 15: Le/h



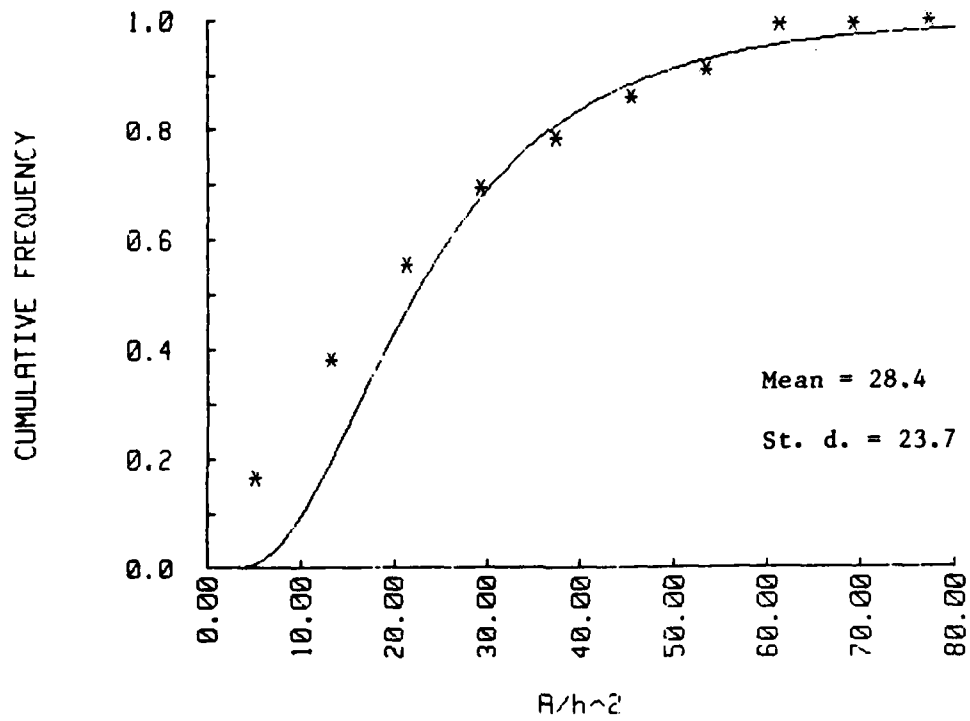
WEDGE TESTS # 13 TO 15: R/h^2



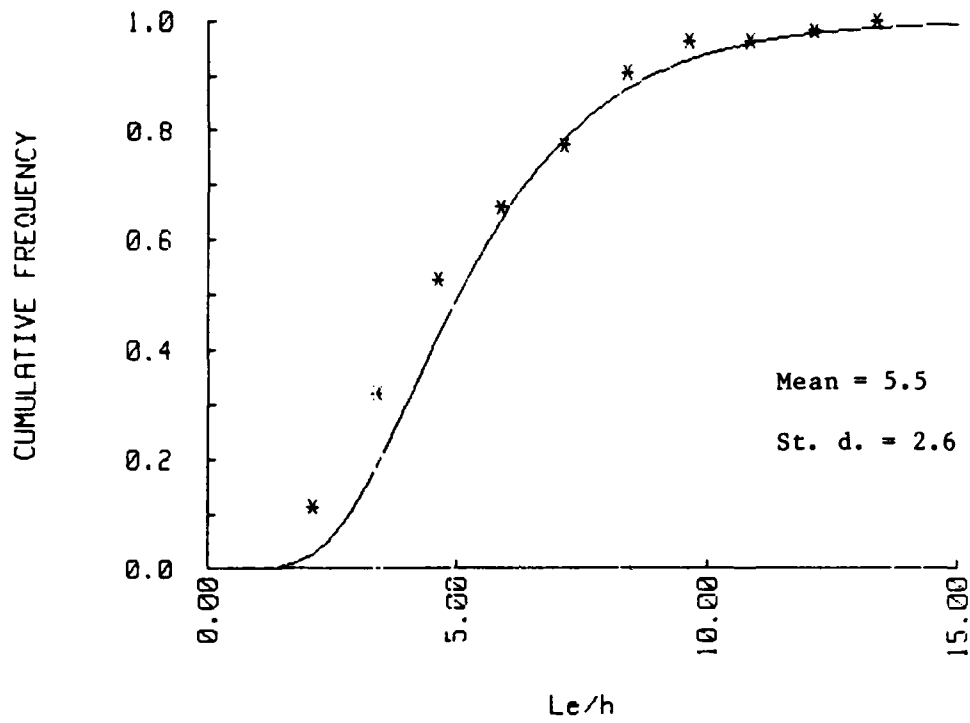
WEDGE TESTS # 16 TO 18: L_e/h



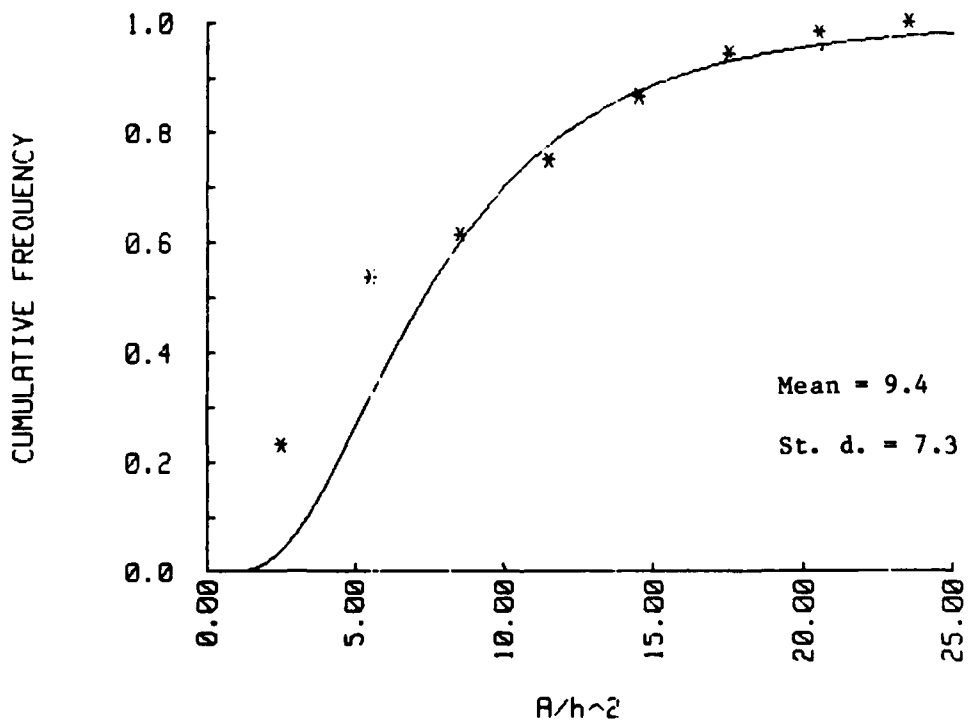
WEDGE TESTS # 16 TO 18: R/h^2



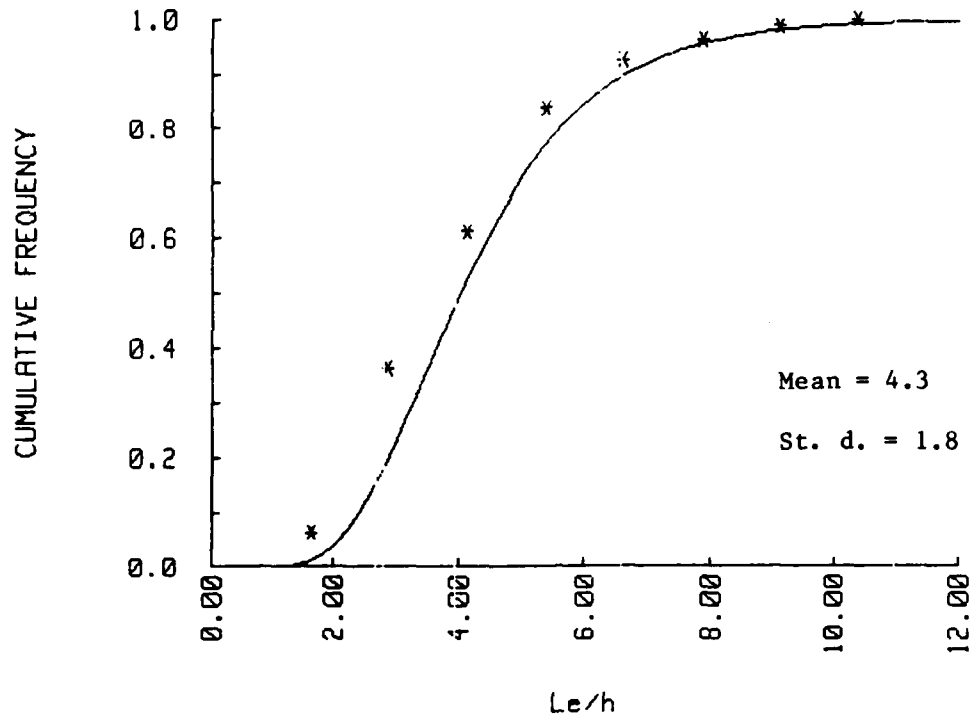
WEDGE TESTS # 19 TO 22: L_e/h



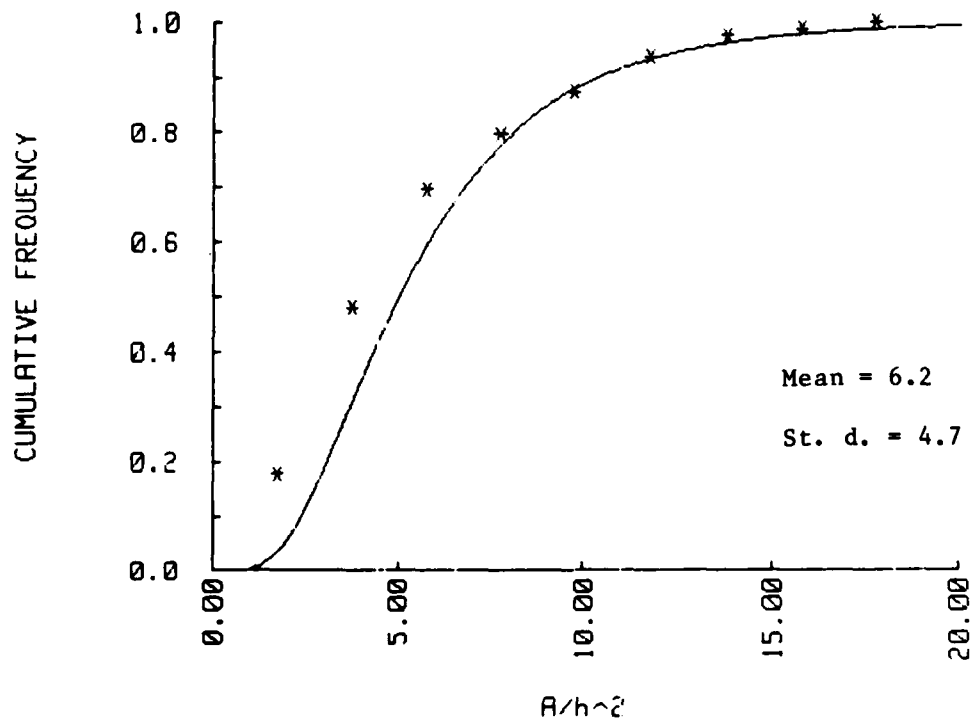
WEDGE TESTS # 19 TO 22: A/h^2



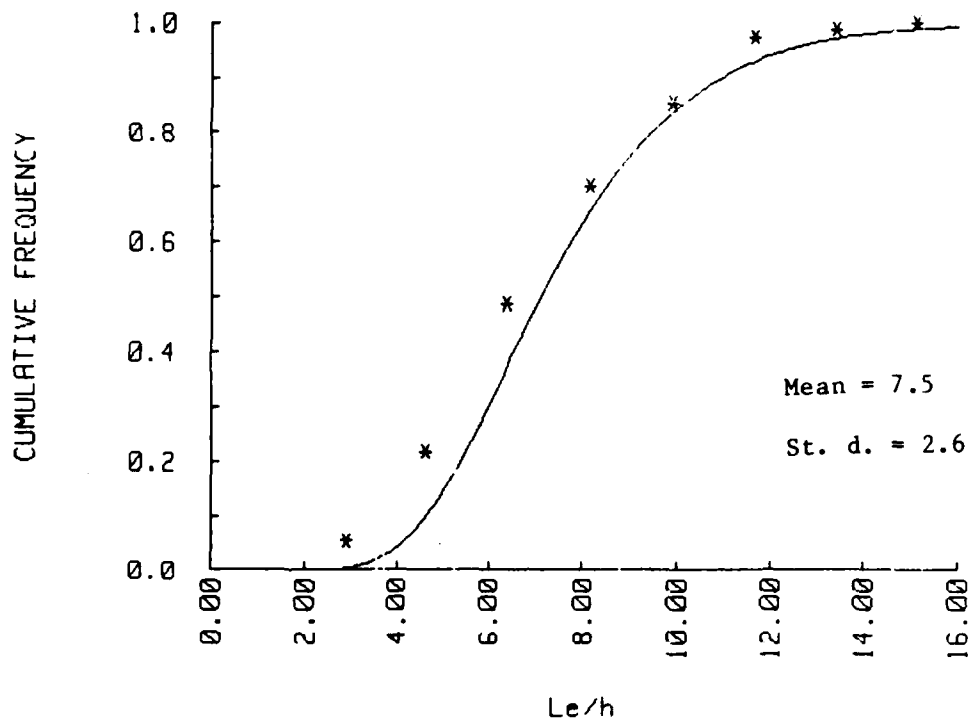
WEDGE TESTS # 23-26: L_e/h



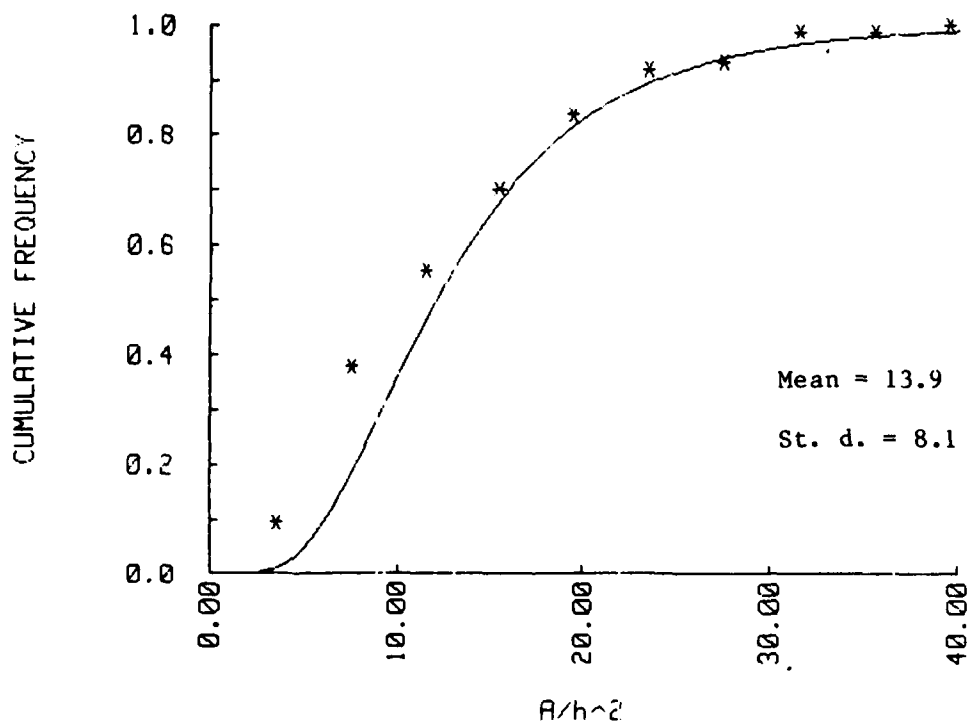
WEDGE TESTS # 23 TO 26: A/h^2



WEDGE TESTS # 27 TO 30: L_e/h



WEDGE TESTS # 27 TO 30: A/h^2



A facsimile catalog card in Library of Congress MARC format is reproduced below.

Tatinclaux, Jean-Claude

Level ice breaking by a simple wedge / by Jean-Claude Tatinclaux. Hanover, N.H.: Cold Regions Research and Engineering Laboratory; Springfield, Va.: available from National Technical Information Service, 1985.

iv, 53 p., illus., 28 cm. (CRREL Report 85-22.)

Bibliography: p. 14.

1. Floe size. 2. Friction factor. 3. Ice breaking. 4. Ice forces. 5. Ice properties. 6. Laboratory tests. 7. Model ice. 8. Probability distributions. I. United States. Army. Corps of Engineers. II. Cold Regions Research and Engineering Laboratory, Hanover, New Hampshire. III. Series: CRREL Report 85-22.

END
FILMED

5-86

DTIC